

POLITECNICO DI TORINO

Department of Electronics and Telecommunications

Master's degree in Nanotechnologies for ICT

Master's degree thesis

Study and realization of optical sensors based on gold nanostructures



Supervisors:

Prof. Davide Janner

Candidate:

Alessio Giuseppe Marino

April 2019

To my family.

I declare that this thesis has not been submitted as an exercise for a degree at this or any other university and it is entirely my own work.

Alessio Giuseppe Marino

Summary

Summary	III
List of figure.....	V
List of tables.....	VII
Glossary	VIII
Abstract	IX
Chapter 1 Introduction	1
1.1 RaPID project.....	1
1.2 Water contaminants.....	2
1.2.1 World Health Organization Guidelines	2
1.2.2 European Union Directive	4
1.3 Raman Spectroscopy	7
1.3.1 Overview of Raman effect and SERS	7
1.3.2 Advantages of Raman.....	9
1.4 Gold Nanoparticles, state of the art	10
1.4.1 Synthesis of gold nanoparticles	11
Chapter 2, Fabrication of substrate and characterization	13
2.1 Fabrication.....	14
2.1.1 Cutting and cleaning procedure	14
2.1.2 Functionalization and seed deposition.....	17
2.1.3 Isotropic growth.....	19
2.1.4 Anisotropic growth: Nanostars	21

Summary

2.1.5 Anisotropic growth: Nanoforest	23
2.2 Characterization.....	26
2.2.1 SEM microscopy	26
2.2.2 UV-visible spectroscopy.....	35
Chapter 3, Analysis with Raman spectroscopy.....	41
3.1 Raman spectroscopy.....	41
3.1.1 Experimental conditions	41
3.2 Contaminants.....	43
3.2.1 Thiram.....	43
3.2.2 Sudan III	44
3.2.3 Carbaryl	45
3.3 Results	46
Chapter 4, Conclusions	55
4.1 Future work	56
Appendix	57
List of chemicals and limits for EU.....	57
Preparation of Growth solutions.....	58
Gold nanospheres.....	58
Gold Nanostars	58
Gold Nanoforest.....	59
Bibliography.....	61
Acknowledgements.....	66

List of figures

Figure 1, Gas chromatography	6
Figure 2, a) Examples of anisotropic gold nanoparticles, b) Spherical gold nanoparticles	11
Figure 3, Process scheme	13
Figure 4, Precision cutter	14
Figure 5, Glass samples obtained from microscope slide	15
Figure 6, a) Bottle with Piranha solution, b) Temperature control	16
Figure 7, Glass surface after cleaning procedure	16
Figure 8, APTMS (3-Aminopropyl) trimethoxysilane	17
Figure 9, Sample surface after Self Assembled Monolayer of APTMS	19
Figure 10, Sample after deposition of Gold seeds	19
Figure 11, Gold nanospheres grown at different times	21
Figure 12, a) DMF, b) PVP	22
Figure 13, Gold nanostars grown at different times	23
Figure 14, Growth process and effect of MBA	24
Figure 15, Gold Nanoforest grown at different times	25
Figure 16, Spherical nanoparticles 3.30 min	28
Figure 17, Spherical nanoparticles, 4.00 min	28
Figure 18, Gold nanoparticles, 4.30 min	29
Figure 19, Gold nanoparticles, 5.00 min	29
Figure 20, SEM image of 10 min Gold nanostars sample	30
Figure 21, SEM image of 15 min Gold nanostars sample	31
Figure 22, SEM image of 20 min Gold nanostars sample	31
Figure 23, SEM image of 5 min Gold nanoforest sample	33
Figure 24, SEM image of 7.5 min Gold nanoforest sample	33
Figure 25, SEM image of 10 min Gold nanoforest sample	34
Figure 26, Light injected is partially reflected, partially transmitted and partially absorbed	35
Figure 27, UV-Visible spectrometer, Shimadzu 2600	36
Figure 28, Experimental set up for UV-Visible analysis	37

List of figures

Figure 29, Absorption spectrum of gold nanospheres	37
Figure 30, Absorption spectrum of Gold Nanostars	38
Figure 31, Absorption spectrum of Gold Nanoforest	39
Figure 32, Comparison between absorption spectrum of Gold nanospheres, Gold nanostars and Gold nanoforest	40
Figure 33, Raman spectrometer, WiTec Alpha 300 RA	42
Figure 34, Thiram, PubChem	43
Figure 35, Thiram Raman spectrum	43
Figure 36, Sudan III	44
Figure 37, Raman spectrum of Sudan III	45
Figure 38, Carbaryl	45
Figure 39, Raman spectrum of Carbaryl	46
Figure 40, Raman spectrum of bare glass	47
Figure 41, Raman spectra of functionalized substrates	47
Figure 42, Raman spectrum of Thiram on several substrates at 100X, 633 nm laser	48
Figure 43, Raman spectrum of Thiram with different concentrations	49
Figure 44, Raman spectrum of Sudan on bare glass	50
Figure 45, Raman spectrum of Sudan on gold nanosphere substrates	51
Figure 46, Raman spectrum of Graphene on glass	52
Figure 47, Raman spectrum of Sudan on graphene and bare glass	52
Figure 48, Raman spectrum of Sudan III on substrates functionalized with Graphene	53
Figure 49, Comparison between Raman spectrum of Sudan III on bare glass, 5.00 min SERS substrate and functionalized graphene substrate	54

List of tables

Table 1, Analytical techniques for inorganic chemicals	5
Table 2, Analytical techniques for organic chemicals	5
Table 3, List of produced substrates	26
Table 4, Average dimension and degree of coverage of Gold nanospheres	30
Table 5, Average dimensions and degree of coverage of Gold nanostars	32
Table 6, Average diameter and Estimate of length for Gold Nanoforest	34
Table 7, List of allowed concentrations for contaminants in EU.....	62

Glossary

APTMS (3-Aminopropyl) trimethoxy silane

AuNP Gold Nanoparticles

CTAB Cetyl-Trimethylammonium Bromide

DMF Dimethylformamide

ETU Ethylen-thiourea

FESEM Field Enhanced Scanning Electron Microscopy

GERS Graphene Enhanced Raman Spectroscopy

LSPR Local Surface Plasmon Resonance

MW Molecular Weight

NATO North Atlantic Treaty Organization

NF Nanoforest

NS Nanostar

NSp Nanosphere

PVP Polyvinylpyrrolidone

RaPID Raman Probe for chemical contaminant Identification

SAM Self Assembled Monolayer

SEM Scanning Electron Microscopy

SERS Surface Enhanced Raman Scattering

TEM Transmission Electron Microscopy

TERS Tip Enhanced Raman Spectroscopy

UV Ultra-Violet

Abstract

The aim of this master thesis is to develop a platform for the detection of organic water contaminants at low concentration by developing a low-cost fabrication process based on wet-chemistry and characterized by high reproducibility.

The thesis has been developed in the framework of RaPID (Raman Probe for chemical contaminant IDentification) project, a project funded by North Atlantic Treaty Organization, division Science for Peace and Security (NATO SPS). Partner universities of this project are Politecnico di Torino, Aalto University and Universitat de Barcelona [1].

The work aims to find an optimum substrate among the several proposed by literature for Raman analysis that should be used as Surface Enhanced Raman Scattering (SERS) substrate. The experiments have focused on glass substrates functionalized with gold nanoparticles. Gold nanoparticles have been chosen because they are known to be a source of Surface Plasmon Resonance (SPR) that allows SERS; the enhanced electromagnetic field generated by these particles allows a dramatic rise in Raman signal coming from contaminants.

Several substrates with different nanoparticles have been tested, such as spherical ones, rod-like grown vertically and star shaped ones. Substrates have been characterized by means of UV-Visible spectroscopy and SEM microscopy. Finally, Raman measures have been performed on Gold nanospheres with Thiram and Sudan III leading to promising results, concentrations of around 20 μM have been easily detected, but further studies are required to validate other substrates and to determine their limit of detection.

The experiments have been carried on in the laboratories of the Department of Applied Science and Technology of Politecnico di Torino, even if several tests have been performed also in the Clean Room of Micronova (Aalto University) and at the Department of Chemistry at Universitat de Barcelona.

Chapter 1

Introduction

1.1 RaPID project

This thesis has been realized in the framework of “RaPID” project, a project funded by NATO SPS (North Atlantic Treaty Organization, division of Science for Peace and Security). RaPID stands for Raman Probe for chemical contaminant IDentification; the goal of the project is to develop a low-cost portable sensor able to perform a rapid analysis of water in order to understand whether organic contaminants are below guard levels imposed by law. Today, this type of control is expensive and time consuming; usually, several litres of water are required, then only a dedicated laboratory with highly skilled operators can perform the analysis, and they require also days. All this cannot be afforded in case of danger, such as a potential contamination due to filters failure of an industry. For this reason, the need for a portable device arises, a sensor that could be used in place, able to give a quasi-real-time answer as accurate as possible, able to detect contamination levels above the safety limits.

The analysis that this sensor has to perform is an optical analysis, label-free. The optical effect that is exploited is Raman effect, moreover due to the weak Raman signal, the sensor will be improved from a gold nanostructured substrate that will provide Surface Enhanced Raman Scattering (SERS) effect.

My work started from the analysis of literature in order to understand the state of the art of SERS spectroscopy to find the best substrate and process that provides the best Enhancement Factor fabricated by wet chemistry, a simple and easily scalable production method. The process used comprises few steps: first the substrate is functionalized to improve gold nanoparticle adhesion, then Gold nanoparticles are deposited and grown in different ways.

Tested substrates include microscope slide glass. The growth step can be realized in different ways, some of them will be detailed later, although two general types can be categorized as:

- *Isotropic growth*: uniform growth of the nanoparticles in all allowed directions leading generally to spherically shaped particles;
- *Anisotropic growth*: direction selective growth following the preferred crystalline planes leading to spiked, elongated or star-shaped particles.

The optimization of the process is oriented to an increase in the surface nanoscale roughness of the gold layer. Indeed, where crevices or points of contact are present in the nanostructured gold surface, a so-called hotspot is formed. In the presence of a hotspot, SERS effect is greatly enhanced up to a millionth time. For this reason, a substrate with high density of hotspots is the final goal to increase sensitivity and time responsivity of the substrate. [6-8].

1.2 Water contaminants

Water is the most important resource on Earth, it allows life as we know, and it is essential for our health as well as for human activities, from agriculture to industrial applications. During the last decades, its quality has been dramatically degraded by several sources of contamination [32-33]. Source of contaminants are everywhere, from air pollution that dilute in water, to industrial residues dumping, from plastic trash that is filling oceans to herbicides and pesticides in underground water due to agriculture. Every source of water shows some degree of contamination, starting from sea water, to underground water and there are many types of contaminants that are dangerous for human health and life in general, starting from heavy metals to herbicides, pesticides and drugs. For this reason, almost all governments have a strict regulation for water quality accordingly to its use, that is regulation differs whether water will be drinkable water, agricultural water etc.

1.2.1 World Health Organization Guidelines

Typically, World Health Organization (WHO) [34] elaborates a series of guidelines to determine water quality, how to perform analysis and which are chemicals and elements that could be dangerous for human life. Then, every government decides how to translate these

guidelines in a legislation; the most important organisms for water legislation are the Environmental Protection Agency from USA and the European Union.

The last release of guidelines from WHO is “Guidelines for Drinking-water Quality” in 2017 [2], they refer specially to drinking water, water that is used directly by humans to drink or for food preparation, so it is the highest quality kind of water, except for water used in specific applications where extra pure water is required.

Guidelines provide a useful reference for risk-management strategies for ensuring safety of water, but also numerical values for hazardous substances that should be kept under control, based on scientific basis. These guidelines should always be applied carefully in the context of a particular region or country, because there is not a universal approach that is worth for every country, each one should generate a legislation that takes into account its peculiar needs.

According to WHO there are three main aspects that should be kept under control to ensure human health:

- 1) Microbiological aspects;
- 2) Chemical aspects;
- 3) Physical aspects.

For what concerns the first aspect, it is related to the presence of bacteria, viruses and helminths in water. Ingestion of these organisms could cause serious intestinal diseases or other type of infections. For this reason, a system of barriers should be used to reduce or eliminate these bodies from water.

On the other hand, there are chemical risks associated to many substances that could be dissolved in water. Typically, a prolonged exposure to these contaminants could cause a serious risk to health; These are of major concern, because when a massive contamination occurs, water becomes undesirable under all aspects, so some purification process is required, and contamination source must be removed.

Finally, there are physical aspects that should be considered. They consist in the presence of radionuclides; a certain amount naturally occurs in water, but presence of high level of alpha and beta radiations should be taken under control.

Guidelines trace also a series of advice about odour, colour and taste about water, because they are fundamental for human perception of safety. Water should appear colourless, without any

smell or taste. Any deviations from these conditions could sign some problem on water treatment and some investigation should be performed.

Of particular importance are the criteria employed to define whether a chemical is dangerous for human health or not. The verbatim definition from [2] reads:

- *There is credible evidence of occurrence of the chemical in drinking-water, combined with evidence of actual or potential toxicity.*
- *The chemical is of significant international concern.*
- *The chemical is being considered for inclusion or is included in the WHO Pesticide Evaluation Scheme (WHOPES) [35], which coordinates the testing and evaluation of pesticides for public health, including those applied directly to drinking-water for control of insect vectors of disease.*
- *Guideline values are derived for many chemical constituents of drinking-water. A guideline value normally represents the concentration of a constituent that does not result in any significant risk to health over a lifetime of consumption.*

According to these guidelines and the scientific community, chemicals could be divided in two categories depending on the effect they could have, those for which exists a threshold below which, also after long exposure, no damages occur, and those that directly act on human DNA, this could potentially cause mutations, hence cancer; for this reason their level should always be below limit of detection of analytical instruments.

1.2.2 European Union Directive

Now it will be exposed how these guidelines have been implemented in the European Union. During 2000 has been published the “DIRECTIVE 2000/60/EC OF THE EUROPEAN PARLIAMENT AND OF THE COUNCIL of 23 October 2000 establishing a framework for Community action in the field of water policy” [3] whose purpose is to establish a framework for the protection of water. It aims to prevent further deterioration of this resource in the Community, reduction of pollution and it promotes protection of aquatic environment. This directive is quite general, and it concerns all types of water and its quality, but there exist several directives specific for drinking water for example, or groundwater, such as “COUNCIL DIRECTIVE 98/83/EC of 3 November 1998 on the quality of water intended for human consumption” which has been updated on 2015 [4].

A crucial point of these directives is monitoring of water quality, this is a key step for assuring that water is clean or that there are dangerous pollutants. This directive states also how and how often the quality of water should be controlled as well as how to retrieve water samples for

analysis, that is in such a way the methodology cannot degrade the sample before analysis and it is representative of the type of water under analysis.

Another crucial point concerning water quality is water disinfection, when water is intended for human consumption, the disinfection process should be verified, chemicals used for this process should be compatible with human life as their by-products.

1.2.3 Analysis methods of water contaminants

The Guidelines from WHO list a series of advanced techniques to perform accurate analysis of organic and inorganic chemicals that is reported:

Table 1, Analytical methods for analysis of inorganic chemicals listed according to complexity

Ranking	Technique
1	Volumetric method, colorimetric method
2	Electrode method
3	Ion chromatography
4	High-performance liquid chromatography
5	Flame atomic absorption spectrometry
6	Electrothermal atomic absorption spectrometry
7	Inductively coupled plasma atomic emission spectrometry
8	Inductively coupled plasma mass spectrometry

Table 2, Analytical techniques for organic chemicals listed according to complexity

Ranking	Technique
1	High-performance liquid chromatography
2	Gas chromatography
3	Gas chromatography-mass spectrometry
4	Headspace gas chromatography-mass spectrometry
5	Purge-and-trap gas chromatography Purge-and-trap gas chromatography-mass spectrometry

Now there will be a simple review of the main techniques to analyse organic compounds [5]:

- Gas chromatography (fig. 1): This technique is exploited for quality control and identification of substances in mixtures. The main principle on which these techniques work is separation of compounds. The analyte is collected by an inert gas flow that bring it in a separation column, here compounds react with a stationary phase, and reactions will be different accordingly to chemicals that are in the mixture. Once they are separated a quantitative analysis could be carried on with several detectors such as Mass spectrometer, Flame ionization detectors... Analysis is influenced by several parameters such as vapour pressure, column temperature, carrier flow rate...
- Liquid chromatography: This technique is based on the same principle of the gas chromatography, but the mobile phase that bring analyte in contact with stationary phase is liquid.

These techniques are extremely precise, and they could detect really low concentrations, but they have several disadvantages, such as the apparatus is definitely not portable, depending on the type of sensor, they could occupy an entire laboratory table as well as a room; moreover, they are extremely sensible and usually, high skilled technicians are required to perform the analysis.



Figure 1, Gas chromatography

For all these reasons the need for easier techniques arises, especially when a rapid and in locus analysis is required. Moreover, the above-mentioned instruments are expensive, so they are not suited for poor countries that cannot afford them, but usually, they are those that need them the most. From this framework arises RaPID project, that aims to develop a portable sensor easy to produce; it is cost effective, several substrates could be produced with a few ml of chemicals, the major concern is the Raman system, but its cost is of the order of thousands Euros, not tens of thousands or hundreds; finally, it is easy to use, it just requires a drop of liquid, some μl , and then, microfluidic circuit and electronics will do everything.

1.3 Raman Spectroscopy

Raman spectroscopy is an analysis technique based on Raman effect that was first discovered by C.V. Raman [36]. This technique is today commonly employed as spectroscopic technique for chemical species analysis; Raman effect is a shift in frequency that undergo a really small fraction of photons that illuminate the sample; due to low signal, it is difficult to detect Raman signal, but today, its success is mainly due to the discovery of the laser and Surface-Enhanced Raman Scattering (SERS), an interesting effect that was first observed in 1973[25]. It consists in a huge increase, several orders of magnitude, in Raman signal when molecules are adsorbed on metal surfaces in certain conditions. In 1997 it has been possible to detect a single molecule thanks to SERS [28], and it was demonstrated that in these particular condition Raman signal could compete with the fluorescence. During last years, a further improvement in Raman instrumentation, but also new nano-fabricated substrates have been essential for the fast development of SERS [29-31]. Has it has been already stated, this work aims to produce a reliable substrate for SERS analysis, based on gold nanostructures. Before the presentation of results that have been achieved, it follows a quick overview of Raman Spectroscopy and SERS effect.

1.3.1 Overview of Raman effect and SERS

When a light beam interacts with molecules, they are put in vibration, this causes scattering of light, that is photons are re-emitted by molecules. The mayor part has the same energy of incoming ones, they undergo Rayleigh processes, that are elastic processes, but a tiny part is subjected to inelastic processes, the final energy will be different with respect to the original

one; these are subjected to Raman scattering, and the immediate consequence is a shift in frequency, this could be positive or negative, depending if they have lost or gained energy. The shift in energy is caused by an interaction between photons and phonons, that are associated to vibration of molecules. In fact, Raman scattered photons are produced by an electronic transition from a virtual state, at which the molecule has been excited by the absorbed incident light, to a vibrational state that is higher or lower in energy than the state from where they started [29]. Therefore, the amount of frequency shift is an indicator of energy involved in the transition between initial and final vibrational states; this is of major importance because the distance between starting and arriving state is characteristic for each molecule, moreover, intensity of Raman signal is proportional to the number of scattering molecules. Unlikely, only a really small fraction of photons is subjected to Raman, usually an intensity of 10^{-6} is observed, which is at least three orders of magnitude below the one of Rayleigh scattered photons, but this problem could be overcome exploiting SERS effect.

SERS is a spectroscopic technique able to obtain signals even from single molecules. It is based on the enhancement of Raman signal when molecules are in presence of metallic nanostructures able to generate Local Surface Plasmon Resonance (LSPR), that is a collective oscillation of surface electrons [29-30]. The amplification of the signals comes (mainly) through the electromagnetic interaction of light with metals, this produces huge amplification of the electromagnetic field through excitations of surface plasmons, but this enhancement could be perceived only in close proximity of metal surface, so it is necessary that molecules that have to be detected are at a maximum distance of 10 nm from metal, better if they are adsorbed on metal surface. In the following I am going to explain qualitatively the physics to capture the most important concepts of SERS. These oscillations on metal surface are caused by the laser beam that acts as external force that excite resonantly the de-localized conduction electrons and they are called plasma oscillations. The resonance frequency of the plasma oscillations that could be associated to quasi-particles, called plasmons, in metal nano-structures depends mainly on the dielectric functions of the metal and the surrounding medium. Because Laser frequency is typically in the range of optical frequencies, a metal whose plasma frequency is in this range is required; the only ones that satisfy this condition are Silver and Gold. The oscillating electric field of incoming laser radiation drives an oscillation of the conduction electrons, leading to a charge separation. This type of resonance is termed dipolar localized surface plasmon resonance (LSPR) and it could be associated to a nano-antenna which can emit radiation at the same frequency of incoming field. This leads to a resonant elastic light scattering and so to an enhanced local electric field that could interact with molecules in close proximity

of metal nanoparticle. The interaction is able to induce a dipole in the molecule and inelastic light scattering can happen. The overall SERS intensity depends on both the “incoming” (W_{inc}) and the “outgoing” ($W_{inc} - W_{vib}$) field. The optimal signal conditions require that both incident field W_{inc} and the shifted one $W_{inc} - W_{vib}$ have to be in resonance with plasmon peak of metal nanostructure. Because each enhancement could bring an increase of E^2 an overall increase of E^4 could be achieved, which is a huge enhancement.

The degree of enhancement of Raman signal is called Enhancement Factor (EF) and large EF are required to detect molecules at low concentration with SERS.

It has been observed and demonstrated that large EF could be reached in the region between two nanoparticles if they are close enough, these regions are the so called “hotspots” [26]. Moreover, it has been observed that hotspots also occur at sharp edges and tips. For this reason, a substrate with high density of hotspots, that means close nanoparticles or nanoparticles with tips would be highly recommended. The EF is made up of not only the electromagnetic contribution, but there is also a chemical contribution, the chemical enhancement due to interaction between the metal structure and molecule that could lead to variations in electronic properties of adsorbates with respect to bare molecules, but its magnitude is much smaller than SERS effect. In its most advanced applications, Raman spectroscopy could reach also single molecule detection, this could be achieved when a nanometric metal tip is employed as probe, this technique is called Tip Enhanced Raman Spectroscopy (TERS) [12].

1.3.2 Advantages of Raman

Raman spectroscopy has been chosen as spectroscopic technique because of its advantages. To name some of them, the fact that there is no need for sample preparation, it requires a small amount of water, some droplet that has to be placed on active substrate, there exist portable Raman spectrometers of reduced dimensions that is fundamental if the aim is to build a portable sensor, the technique works finely in a wide range of conditions, it does not require vacuum or particular temperatures. Moreover, the analysis is fast, according to setting parameters, a few minutes are enough for a measure. Finally, because this work deals with water-based solutions, in the range of frequencies of interest, there is no Raman signal, water is transparent, this creates a perfect condition for detecting contaminants [37-38].

1.4 Gold Nanoparticles, state of the art

For the purpose of this work, substrates based on gold nanoparticles have a great importance, because from its quality will depend quality of Raman signal; for this reason, a brief review of state of the art on gold nanoparticles is provided [6][39-40].

During years, the scientific community have devoted many efforts through gold nanoparticles, they are extremely fascinating due to their potential uses, such as in the field of sensors, catalysts, drug carriers, imaging agents and so on thanks to their amazing physical, optical and chemical properties as their structures [6].

When dealing with nanoparticles, usually, precise control of morphological features is required. For this reason, an uncountable number of production methods have been developed that allow to have very different shapes from nanospheres to branched nanoparticles [6-8] (fig. 2). Lots of efforts are devoted to find ways that avoid the use of lithography because of its cost. Due to this, research is going in the direction of wet chemistry or electrochemistry. These methods are more difficult to control because they are based on chaotic processes and it is difficult to achieve only one well defined type of nanoparticle, but usually, their shape and dimensions follow a certain distribution. The goal is to determine reagents and process conditions that minimize the amplitude of this distribution.

When dealing with these processes there are many parameters that could be controlled, to name some, pH of reacting solution, temperature, concentration of reagents, reaction time, while parameters that characterize nanoparticles that has to be controlled is size, branching, shape; these are essential parameters because they deeply influence the answer to external stimuli, such as plasmonic characteristic.

Today there exist many optimized processes to produce gold nanospheres, gold nanorods, nanocubes, while it is still difficult to produce with high accuracy branched nanoparticles or nanoforests. There is a lot of interest in the last class of nanoparticles because of their high surface roughness, possible high-index facets and large surface-area-to-volume ratio, they may be utilized for surface-sensitive applications such as sensor or catalysts. In this thesis, they are studied because of optical properties, in particular, the LSPR effect, Local Surface Plasmon Resonance, that make them ideal for SERS.

The main strategies for nanoparticle growth, in the framework of wet chemistry methods, are the “seed mediated growth” and “seedless growth”. This work is focused on the first method because it yields better results. Moreover, usually, these particles are prepared in colloidal solutions, then particles are filtered, and, at the end, they are deposited on a functionalized substrate. Within this thesis, another approach has been followed, the main idea is to improve the number of nanoparticles on glass surface, so instead of attaching particles that are grown in colloidal solutions, seed are first attached on glass and then they are grown. This has also another advantage, which is to eliminate filtering stage. This method is expected to work because when dealing with huge nanoparticles there are stronger repulsion forces between them, this reduces the final density on glass substrate, while this could be avoided with a direct attachment of seeds. A drawback of this methodology is that the initial quantity of gold on glass cannot be controlled, and this is one of the parameters that influence growth of nanoparticles.

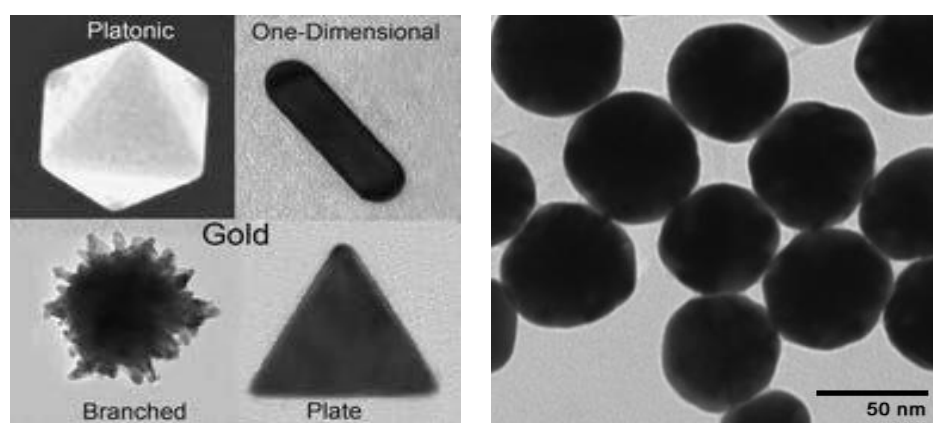


Figure 2, a) Examples of anisotropic gold nanoparticles, b) Spherical gold nanoparticles

1.4.1 Synthesis of gold nanoparticles

When dealing with synthesis of metal nanoparticles many parameters and ingredients could be controlled to have the desired result. Among them of great importance are:

- reactivity of metal precursor: this is important with anisotropic nanoparticles, this effect in fact is exploited because different reticular plains will react differently with the same chemical;
- surface effect of capping agent: it is a reagent that binds to the nanoparticle preventing growth, it will bind in a different way according to plain, allowing the particle to grow in different ways according to direction;

- gold source: this is a gold precursor, when dealing with gold, it is typically Tetrachloroauric acid. When it is in solution it is in the form of Au(III) so it is required a reducing agent to form metallic gold;
- the reducing ability of reducing agent: reducing agent is a reactant that reduces metal ion to metallic form in such a way it could deposit on seed;
- reaction temperature: usually, it is room temperature;
- concentration: this is a key parameter, concentration of reagents is often the key for controllable and reproducible processes;
- reaction time: also, this parameter is important, it controls the size of particles;
- catalysts and additives: these are co-reactants that help controlling reactions.

One of the most famous seed mediated methods for production of gold nanorods is the one developed by Murphy [41-42] based on the use of CTAB, Cetyl-trimethylammonium bromide, a surfactant; the head group of CTAB would bind preferentially to {100} faces of gold, hence, the seed grows longitudinally along {111} faces. In order to develop sustainable production processes, organic surfactants and macromolecules have been also employed, such as DNA that could be employed as a template [43].

Talking about seedless methods, they have the advantage to be versatile and easy to reproduce, but they are highly sensible to process conditions, leading to difficulties in controlling shape and size. Wang and Halas [44] reported nanoparticles with meat-ball morphology made by reaction of chloroauric acid and AA. Branched flowerlike gold nanocrystals were obtained through one-pot synthesis using N0-hydroxyethylpiperazine-N0-ethanesulphonic acid (HEPES) as both reducing and stabilizing agent [45]. To improve synthesis efficiency biomolecules have been employed such as amino acids, peptides and proteins.

There are several other ways to produce gold nanoparticles, that employs always a wet chemical route, but they involve also electrochemistry, as demonstrated by Wang [46]. In a typical set up, an electrode is made of gold while the counter-electrode is in platinum, while the electrolyte solution contains surfactants to prevent aggregation and to allow anisotropic growth. The gold electrode is gold source while reduction happens in proximity of platinum electrode while a silver plate is introduced. Adjusting the process conditions, such as voltage and reactants in solution it is possible to change the morphology of particles, in particular, highly branched and dendritic structures could be achieved.

Chapter 2, Fabrication of substrate and characterization

In this chapter, the fabrication process of all substrates will be discussed and how they have been characterized by means of UV-visible spectrometry and Scanning Electron Microscopy.

All the processes and chemicals that have been employed will be detailed, starting from cleaning procedure to growth processes. A general view of the process is depicted in the scheme below (fig. 3).

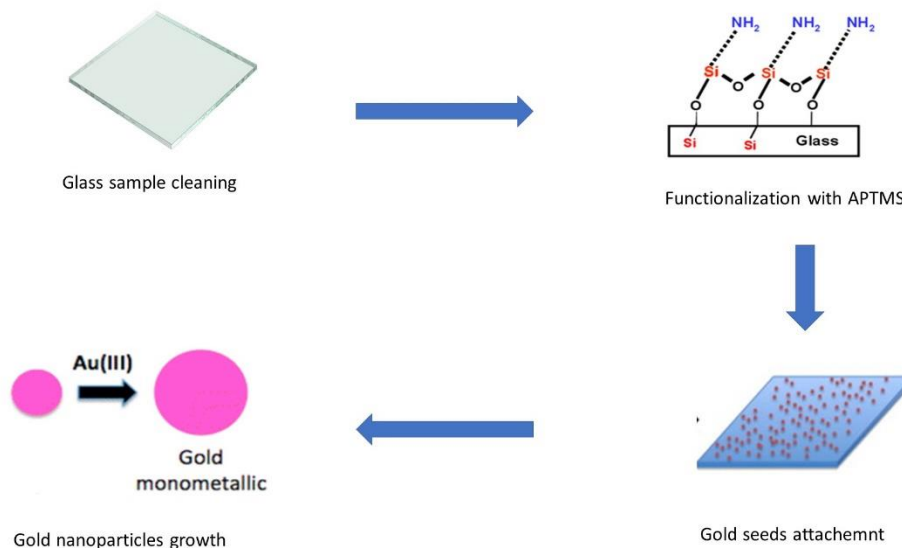


Figure 3, Process scheme

2.1 Fabrication

It follows a detailed view of production steps required to produce the substrates, from cutting of samples to gold seeds deposition and their growth.

2.1.1 Cutting and cleaning procedure

The glass samples have been retrieved from microscope glass slides, from AmScope. The slide has been cut in 14 pieces of around 1 cm² as shown in the figure, with a precision cutter (fig. 4-5). The pieces have been first cleaned with acetone and ethanol, then they have been stored in a sterile plastic bag until use.

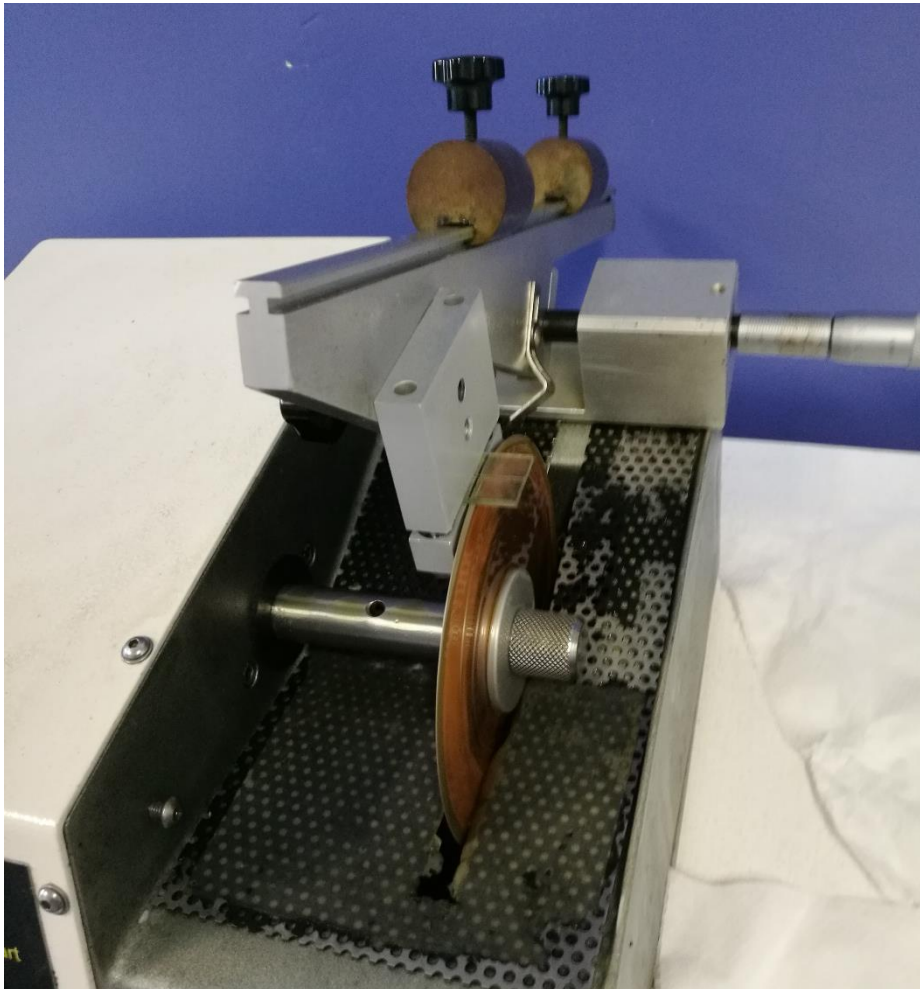


Figure 4, Precision cutter

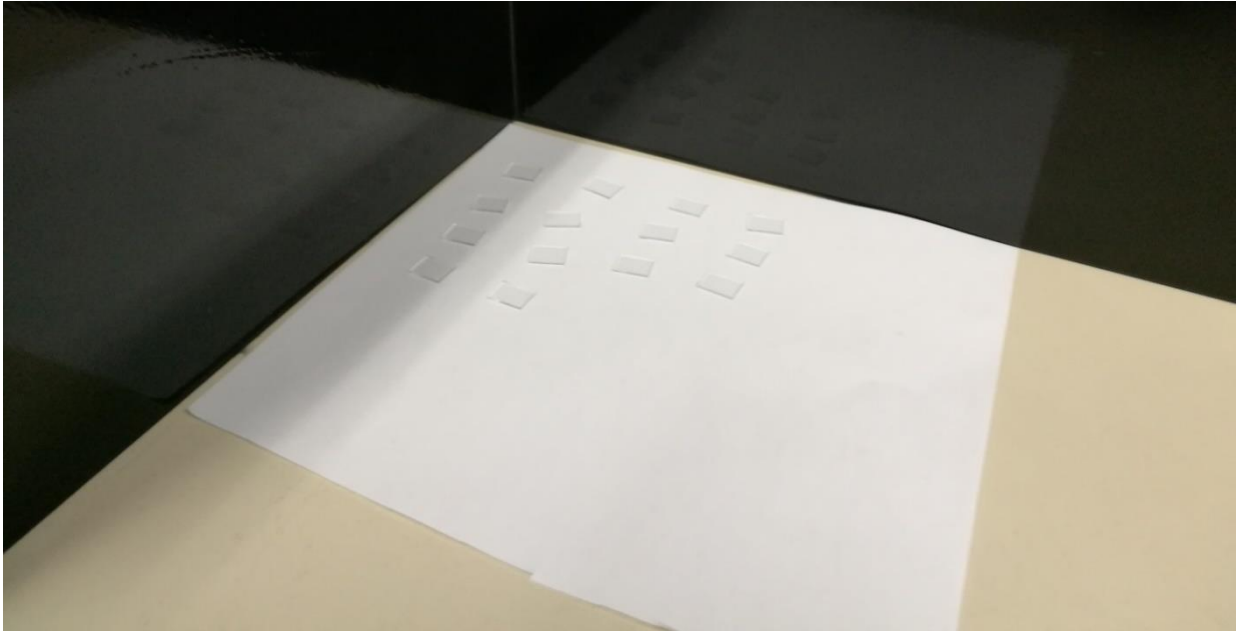


Figure 5, Glass samples obtained from microscope slide

Before any treatment, a strong cleaning procedure is necessary to remove any organic residue from glass surface [47]. At this stage two options arise:

- 1) Plasma Cleaning;
- 2) Piranha.

The first option would be the best, because it provides a set of parameters that are more controllable, so it is easier to set them in such a way to remove organic traces but leaving unchanged glass surface. Unfortunately, this option was not feasible in Turin, due to some problem with Plasma cleaner, so the first way has been chosen. In order to have a solution not too aggressive, it has been decided to use a basic piranha [9], this has the property to be less aggressive than the acidic counterpart. An important result expected from cleaning procedure, above removing organic compounds from surface, thanks to Piranha strong oxidizing power, is to hydroxylate glass surface, that means adding OH groups, it makes surface strongly hydrophilic, a fundamental passage to allow APTMS to attach to Silicon atoms (fig. 7).

Starting with the procedure, a pre-cleaning has been operated on the samples, it consists of acetone bath than two consecutive ethanol baths, both from Carlo Erba Reagents, then samples have been immersed in MilliQ water until the Piranha solution was ready.

The basic piranha is formed by MilliQ water, hydrogen peroxide 35% (from) and ammonium hydroxide (% from), with proportions 7:1:5 in order and it is brought to 60 °C to activate reactions; samples are put in the solution when it reaches this temperature and they are treated

for 30 minutes. 25 ml of solutions have been prepared in a glass bottle while temperature was kept under control with a thermometer (fig. 6). After cleaning, samples have been washed repeatedly with MilliQ water and sonicated in water for 5 min to eliminate excess reagents, finally they have been stored in fresh MilliQ until the following treatment.

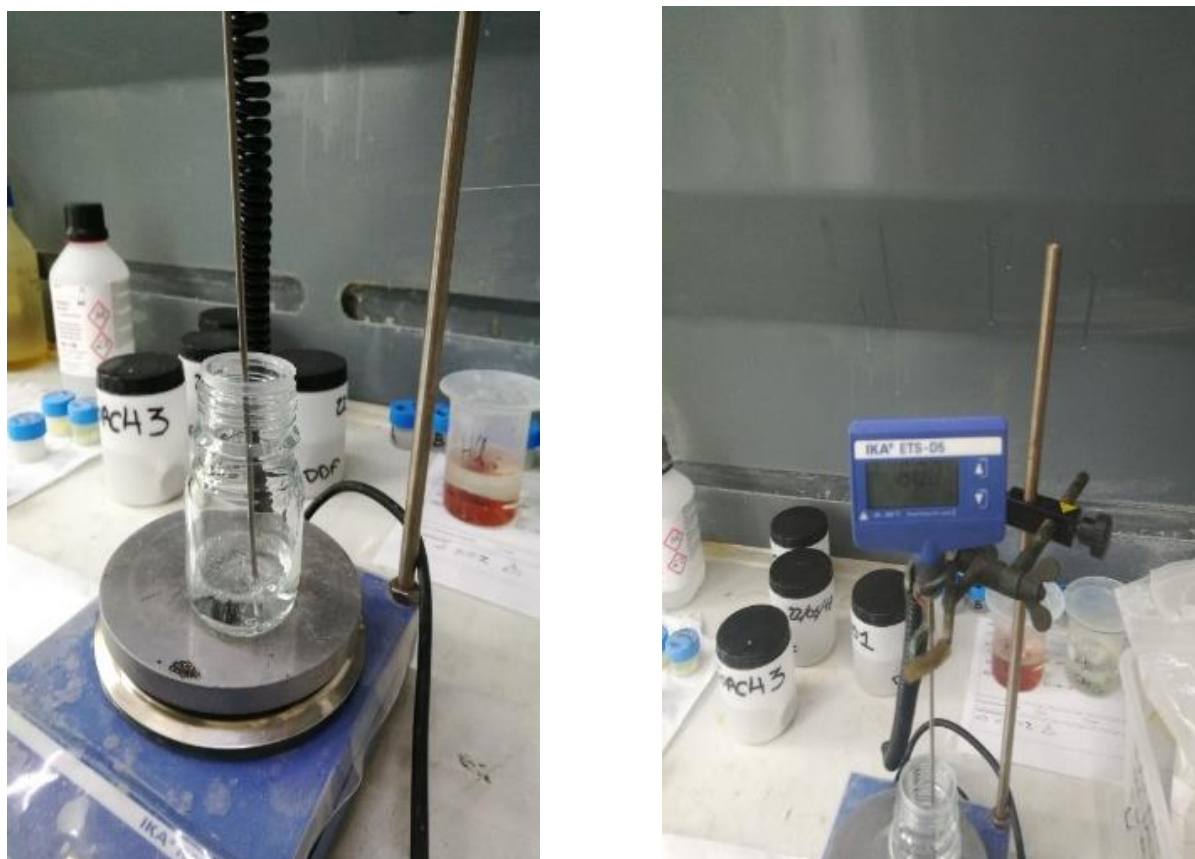


Figure 6, a) Bottle with Piranha solution, b) Temperature control

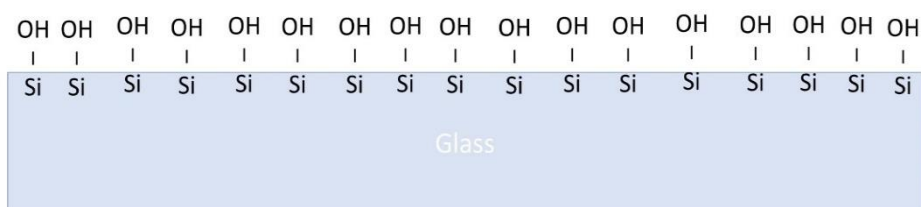


Figure 7, Glass surface after cleaning procedure

2.1.2 Functionalization and seed deposition

The functionalization procedure consists in a surface modification of glass, it is required an agent that chemically binds to glass on one side and to gold seeds on the other side. The idea is to deposit a SAM, Self-Assembled Monolayer, an innovative procedure that allows to deposit only one layer at time, because the reaction is self-limited, this makes this technique really controllable and it provides really uniform layers [48-53]. In this case, according to the work of Karl Meissner [16], from which this thesis has started, among several type of aminosilanes, APTMS (fig. 8) has been chosen because it provides the highest density of gold seeds attached. It is (3-Aminopropyl) trimethoxysilane and it owns to the family of aminosilanes, they are characterized by a Silicon atom and ammine groups. The Silicon atom will bind covalently to glass forming a Si-O-Si bond, while amine groups will bind to gold. For this reason, a glass surface perfectly cleaned is necessary, to have a uniform layer of APTMS and to avoid holes after gold deposition. The process of depositing a Silane compound on glass is called Silanization [52], the hydroxyl group (-OH) on glass surface will attach to alkoxy group in the silane, this complex will be displaced, and a Si-O-Si covalent bond will form (fig. 9).

According to the procedure developed by Meissner, a solution of 2.5 % in weight of APTMS (from Sigma-Aldrich) in Ethanol has been prepared. Each sample has been treated separately, so in a falcon 4 ml of solution have been poured. All these operations should be executed under chemical hood to avoid that APTMS goes in contact with humidity, because this could degrade the chemical.

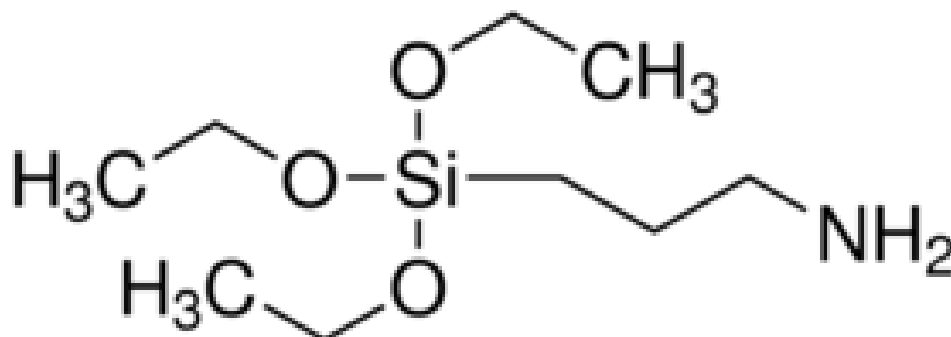


Figure 8, APTMS (3-Aminopropyl) trimethoxysilane

As demonstrated by Messner, this SAM layer keeps the roughness of surface close to the one of bare glass; a lower amount of APTMS would not be sufficient to produce a uniform coverage of glass surface, while a greater one would lead to formation of clusters.

After the cleaning procedure, it is necessary to dry water from samples, it should be done with a Nitrogen flow or under hood at maximum speed in such a way dust cannot deposit on cleaned surface. After that, the sample is completely immersed in the solution with closed plug for 2 hours.

After this time, another cleaning procedure is required to remove excess APTMS from glass surface. In this case it is done by a bath and sonication in Ethanol for 5 minutes, then a further bath in Ethanol; afterwards, another drying step is required, as before, with a Nitrogen flow or under hood at maximum speed, this would be much faster because Ethanol evaporates quite easily.

After this step, it is time for attaching gold seeds (fig. 10). In all the experiments that have been carried on for this thesis, 10 nm AuNp in citrate-buffer have been used and they have been purchased from Sigma-Aldrich. The solution shows the characteristic colour of gold nanoparticles of this dimensions, which is a weak red [54]. Because of their relevant cost, each falcon has been filled with 3 ml of AuNP solution, then the functionalized glass samples have been immersed in the solution overnight, typically 21 hours, from 12.30 to 9.30 of the following day. After seed deposition, samples have been washed again, first with Ethanol, then, twice with MilliQ water. After this process, they are no more completely transparent, but they show a weak pink, that means that seeds have successfully attached to APTMS. The samples have been stored in MilliQ water until the following treatment took place.

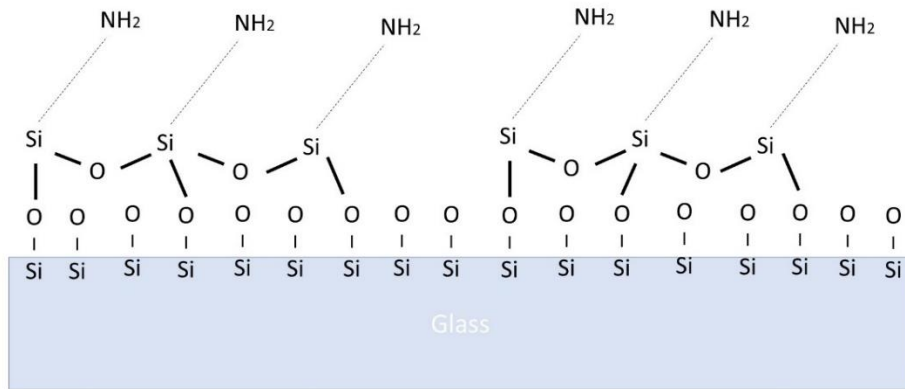


Figure 9, Sample surface after Self Assembled Monolayer of APTMS

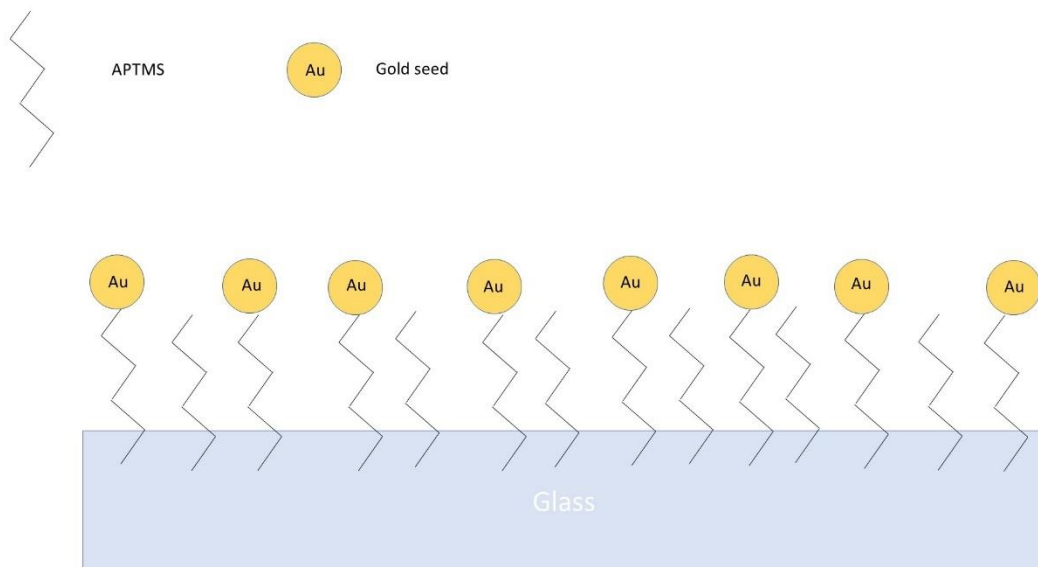


Figure 10, Sample after deposition of Gold seeds

2.1.3 Isotropic growth

The first type of growth that has been developed, following the work of Messner [16][17], it has been isotropic growth, that means if seeds are spherical, growth process keeps the original

shape, growth should be the same in all directions, hence final particles will show a spherical shape.

The process is quite simple and fast, it involves just Tetrachloroauric acid trihydrate and H_2O_2 that activates reduction reactions to bring Au^{III} to Au^0 that will deposit on seed surface. In this work several reaction times have been tested in order to understand how particles grow with time and whether dimensions influence Raman response. This is expected because as particles grow, the interparticle space reduces, enhancing the possibility for analyte molecules to reach a hotspot.

This procedure works with several pH conditions, producing different shapes. It has been demonstrated [55] that working in weak acidic conditions leads to quasi-spherical particles, where H_2O_2 acts as reducing agent, gold seeds as catalyst and $\text{HAuCl}_4 \cdot 3\text{H}_2\text{O}$ as oxidizing one. Gold seeds, acting as catalyst speed up reaction, the new formed Au^0 will fast and selectively deposit on seeds, reducing the production of new particles.

The growth solution should be 0.28 mM of $\text{HAuCl}_4 \cdot 3\text{H}_2\text{O}$ in MilliQ water with 1.75% in volume of H_2O_2 . Each sample has been treated separately, so 5 ml of solution have been poured in each falcon. An important aspect is the fact that because H_2O_2 activates the reduction reaction, it should be added after the glass sample has been immersed in solution; moreover, a vigorous magnetic stirring is required to help mixing all chemicals. It is possible to understand that the reaction is taking place when glass samples start changing colour, from almost transparent to a uniform light pink.

Before this treatment it is required to dry glass samples as in the previous steps. After treatment, in order to stop reactions, samples are immersed in MilliQ water and repeatedly washed with it to remove excess reagents. Finally, they are dried in the hood to remove all water from its surface. At this stage they could be stored in a clean and dried sample holder up to analysis.

For these set of samples, the set of times that have been studied are:

- 3.30 min
- 4.00 min
- 4.30 min
- 5.00 min

The result could be seen in the image below (fig. 11).



Figure 11, Gold nanospheres grown at different times

From the photo it is possible to see the result of this process, glass samples show a weak pink-violet colour, the growth is not extremely uniform across the sample, but it is quite even in terms of holes. The region where a major growth is present is the one along the edge of stirrer, it could be recognized from the round shape, this means that kinetics of fluid covers an important role for this process, and a more uniform result could be achieved exploiting a different way to mix the fluid. Ideally as time of reaction goes on, the colour should be stronger because particles are growing, so a greater region is covered; this is usually respected, even if it also depends on initial density of gold seeds on surface. As it could be seen in the last case, the sample on the right seems clearer, this could be led to a not perfect cleaning before seed attachment, thus less seeds, less growth. In any case it is difficult to determine the dimension merely from colour with naked eye, so a deeper analysis with Uv-Visible spectroscopy and Electron Microscopy have been performed.

2.1.4 Anisotropic growth: Nanostars

The second type of growth is an anisotropic growth. As stated before, anisotropic nanoparticles are expected to give a better Enhancement Factor because, above hotspot effect, also field enhancement due to tips should be present. So, two types of anisotropic nanoparticles have been grown. Starting from nanostars, they are particles that are supposed to have many tips. The process that has been followed is the one of Marzan and co-workers [19][56], it exploits Polyvinylpyrrolidone (fig. 12) as both capping agent and reducing agent dissolved in Dimethylformamide and Tetrachloroauric acid trihydrate as source of Au. PVP is able to control reduction kinetics of AuCl_4^- . The key factor of this process is that the concentration of PVP is

high compared with similar works. At lower concentrations the result are particles much more uniform in shape. The process that has been implemented in this case is slightly different from the one developed in the reference article; it develops gold nanostars in a colloidal solution, while in this research the same process has been tried starting from gold seed fixed on a substrate.

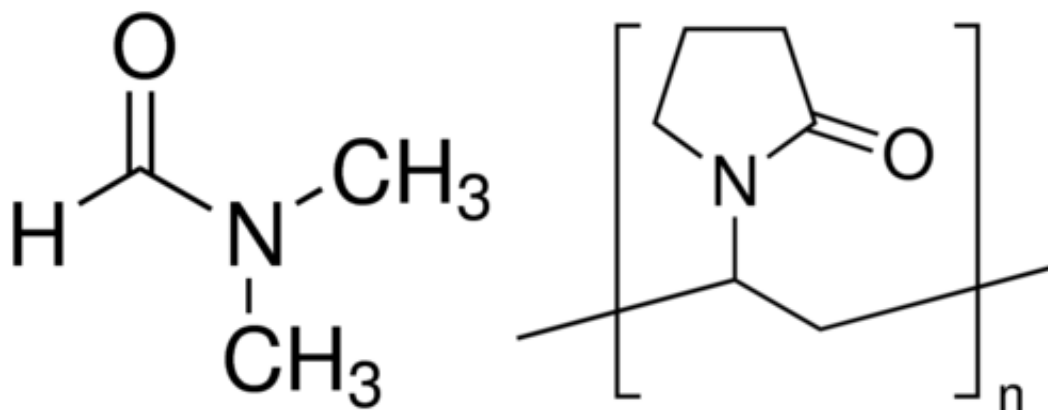


Figure 12, a) DMF, b) PVP

For this experiment, the solution has to be 10 mM of PVP in DMF and it has been prepared first; 4 ml of DMF and 400 mg of PVP (10000 M.W. from Sigma-Aldrich) have been added in each falcon and the solution has been stirred for several minutes to have a homogeneous one. Then, previously dried glass samples have been completely immersed in solution and finally, 22 μ l of a solution 50 mM of $\text{HAuCl}_4 \cdot 3\text{H}_2\text{O}$ in MilliQ water have been added. The final solution has been stirred for the whole duration of treatment; the treatment is working in the right way if after 7 minutes the solution starts changing colour, it becomes of a dark blue, as glass surface. As in the previous case, to stop reactions, the sample has been immersed in clean MilliQ water and then repeatedly washed with MilliQ water and finally dried and stored for analysis.

In this experiment, effect of time on nanoparticles growth have been indagated; 3 different times:

- 10.00 min
- 15.00 min
- 20.00 min

The final result is shown in figure 13. At a first sight the samples show a light blue colour; this is a first sign that particles that have grown are branched, this means that an anisotropic growth

took place, as expected. As in the previous case, the layer shows darker regions, but there are no holes, except a sample in the first set, but in this case, it was not completely immersed in the growth solution, for this reason there could have not been growth. From the picture it is possible to see that for this process, time is a key factor, in fact the substrates show a more intense coloration as time goes on. From experiments, it has been seen that an appreciable change in colour happens around 8-9 min, so coherently, the 10 min sample is the lighter, then samples are always darker.

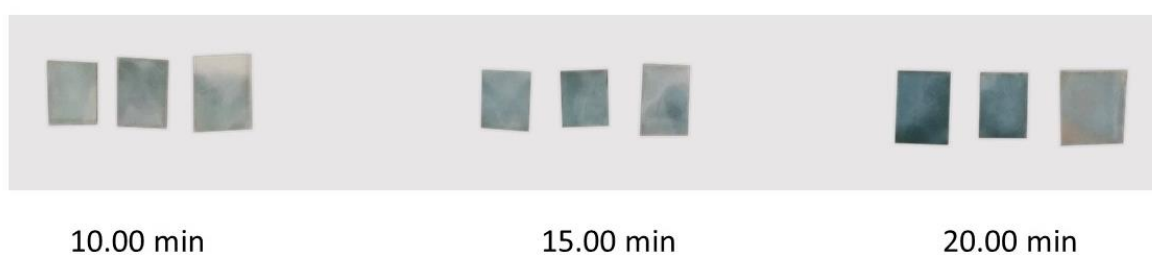


Figure 13, Gold nanostars grown at different times

2.1.5 Anisotropic growth: Nanoforest

The final case that has been studied is growth of a gold nanoforest made by several vertical nanowires, following the work of Y. Wang and J. He [20][57]. Seeds have been grown in such a way seeds have developed vertically. This type of growth is expected to enhance signal because particles touches in many points, hence the number of hotspots should be higher. This type of process is a bit more complicated with respect to the previous ones because it involves more chemicals. In this case, there is the 4-Mercaptobenzoic acid that acts as capping agent, it will cover gold structure as it grows, preventing isotropic growth along sides, then there is L-Ascorbic Acid that is the reducing agent, finally there is $\text{HAuCl}_4 \cdot 3\text{H}_2\text{O}$ which is the source of gold.

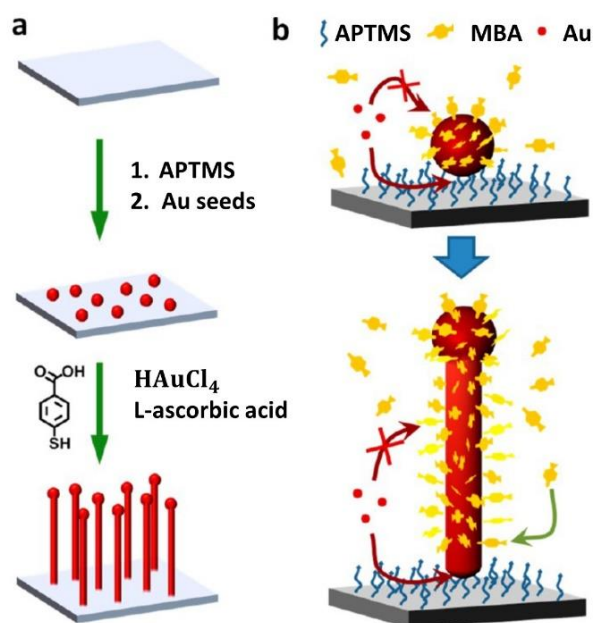


Figure 14, Growth process and effect of MBA

The idea of this type of growth is that MBA, the capping agent, covers all surfaces available of gold (fig. 14), except the one in contact with APTMS, the lower one and as the growth goes on, MBA keeps covering the new surface that is generated, but not the one mentioned before, so the growth goes on until it is stopped or the gold is consumed or the reaction is stopped. The seed will be lifted on as process goes on. In this case, a substrate is necessary to grow the forest, otherwise seeds will grow in all directions at a reduced rate due to MBA. For what concerns the diameter, it will strongly depend on the ratio MBA/Au, while it is nearly independent of gold seed dimension. Experiments have shown that the higher MBA concentration, the lower the diameter. In the opposite case, wire will be always thicker, until a uniform layer is formed. But, in this process, the diameter will increase if more gold will be supplied, and this happens increasing concentration of $\text{HAuCl}_4 \cdot 3\text{H}_2\text{O}$ and the reducing agent, L-AA; so, it is possible to say that diameter is a trade-off between how fast MBA binds to the wire and gold that is reduced. Differently from CTAB driven processes, in which CTAB binds on specific facets, hence growth happens along specific directions, in this case, the growth does not follow specific directions.

Before preparing growth solution, it is necessary to prepare a solution 550 μM of MBA (Sigma-Aldrich) in Ethanol, then a solution 1.7 mM of $\text{HAuCl}_4 \cdot 3\text{H}_2\text{O}$ in MilliQ water and finally a solution of 4.1 mM of L-AA(Sigma-Aldrich) in MilliQ water the base solution is 3:1 in volume of Ethanol and MilliQ water, then the other components are added in such a way molarity is unchanged; they have to be added following a precise order, otherwise the process will not

work: first 578 μL gold solution is added, then dried glass samples are immersed, after that 40 μL of MBA and finally 40 μL of L-AA. It is important to add at the end L-AA because it will activate reduction reactions, hence if it is inserted before MBA, a different growth will start. It is necessary to stir the solution for some second after adding L-AA to mix all components, then, stirring could be turned off, reactions will keep on until the sample is removed; the process is working if glass sample turns to a dark grey within the first minutes. As previously, the reaction ends when the sample is put in MilliQ water and then washed repeatedly and dried.

In this case, three different growth times have been analysed:

- 5.00 min
- 7.30 min
- 10.00 min

And the final result is the one depicted in figure 15.

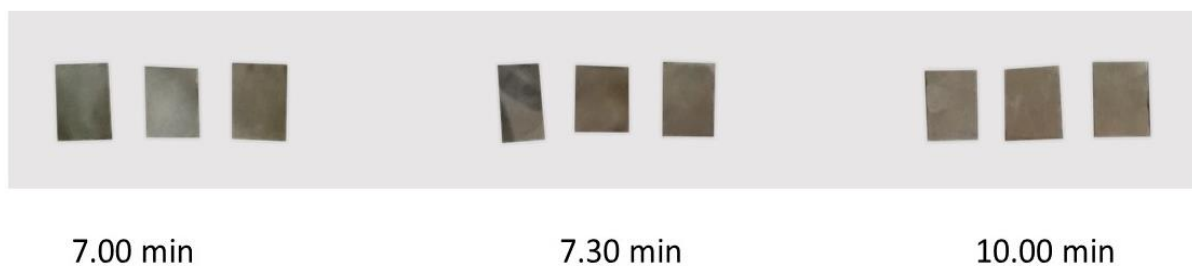


Figure 15, Gold Nanoforest grown at different times

From the figure above, it is possible to see the result of this last process, the samples show a dark grey colour. In this case, the treatment has been much more uniform, this could be led to the fact that stirring is stopped in a few seconds, instead, for what concerns the effect of time, it covers a minor role with respect to other types of growth, in fact there is no such an appreciable difference between different samples grown at different times, but a deeper analysis has been carried on.

Table 3, List of produced substrates

Typology of growth	Time
Gold nanospheres	3.30 min
	4.00 min
	4.30 min
	5.00 min
Gold nanostars	10.00 min
	15.00 min
	20.00 min
Gold nanoforest	5.00 min
	7.30 min
	10.00 min

2.2 Characterization

In this section it will be described how characterization of samples has been performed, first by means of SEM microscopy and then UV-Visible spectroscopy.

2.2.1 SEM microscopy

A first type of characterization has been performed exploiting Field Enhanced Scanning Electron Microscopy. Gold nanospheres have been analysed at Aalto university with Zeiss FESEM at 5 kV with InLens mode. For what concerns nanoforest and nanostars, analysis have been carried on in Barcelona. The purpose of this analysis is to study the morphology of substrates, to understand whether the synthesis has been successful or not and to determine final dimensions of grown particles and final surface density.

Scanning electron microscopy [58-59] is an advanced technique for analysis and characterization of materials, based on a beam of electrons focused on a spot. It can reach a resolution of some nanometres easily. It is based on collection and analysis of electrons that have interacted with matter, hence have been deviated; this allows to build an image of matter. The study of energy of these electrons as well as photons emitted by matter due to interaction with electrons allows also a characterization of the material. If materials are not conductive it is necessary to deposit a thin layer of conductive material to avoid charging effect, that is electrons that are not redistributed in the material, start to shield with their negative charge the electrons flow [60]. Within these experiments there has been no need for metal coverage

because we are dealing with metal nanoparticles. Field enhancement is a type of SEM microscopy that provides better image quality due to increased number of electrons produced by a metal tip that undergoes huge fields.

Images have been analysed with software ImageJ [21], a Java based software released by National Institute of Health of United States. This has been used to determine dimension of nanoparticles and to determine degree of coverage in case of spherical nanoparticles and nanostars, as well the average diameter and average length of gold nanowires.

Starting from gold nanospheres, from images below it is possible to see that as time goes on, particles keep growing; in the last case, at 5.00 min, it is possible to see that coalescence start to be important, that means particles are merging (fig. 16-19).

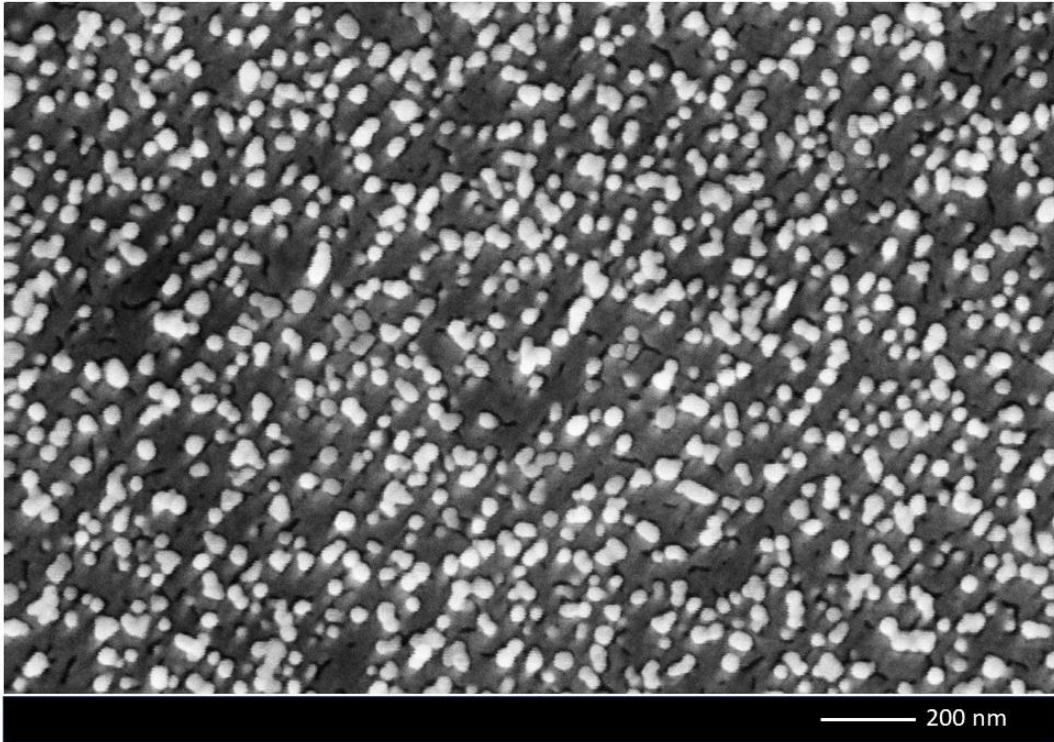


Figure 16, Spherical nanoparticles 3.30 min

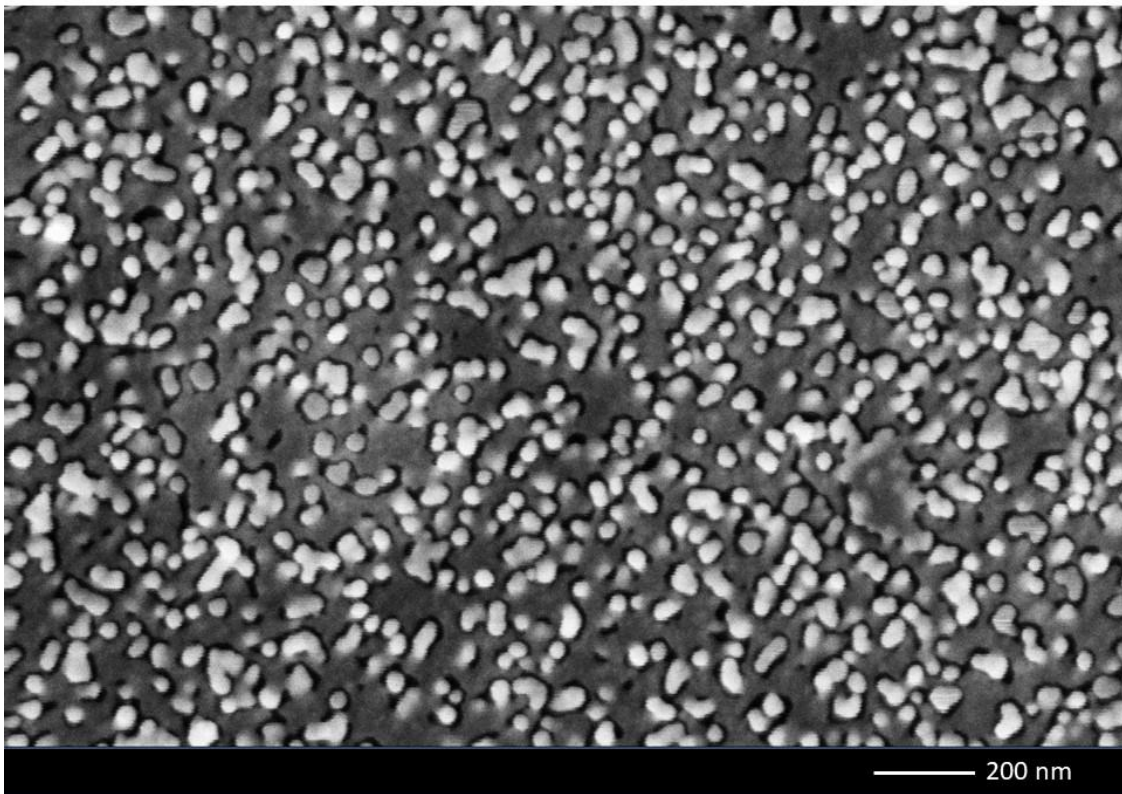


Figure 17, Spherical nanoparticles, 4.00 min

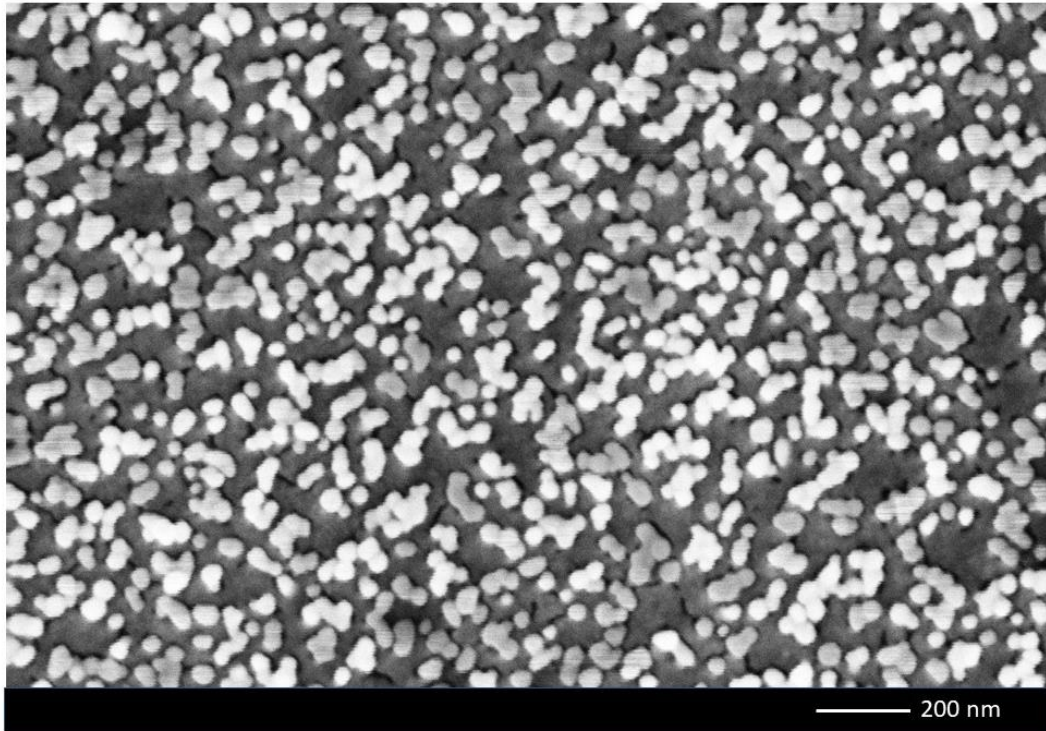


Figure 18, Gold nanoparticles, 4.30 min

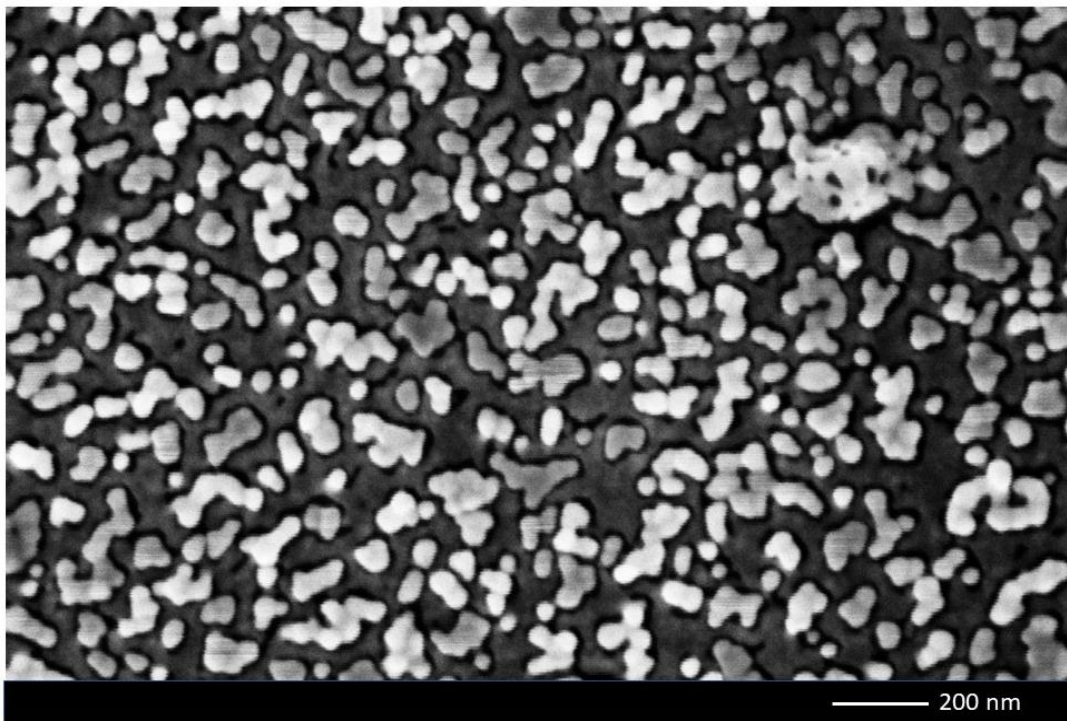


Figure 19, Gold nanoparticles, 5.00 min

Table 4, Average dimension and degree of coverage of Gold nanospheres

Growth time	Average dimension	Degree of coverage
3.30 min	37 nm	30 %
4.00 min	50 nm	35 %
4.30 min	53 nm	39 %
5.00 min	65 nm	43 %

Moving to nanostars, three SEM images are reported below (fig. 20-22), they correspond to one image for every sample grown at different times. In this case it has not been possible to reach a high resolution due to strong charging effect, except for the last case, where particles are larger, so this effect is mitigated by their metallic nature. At a first sight they seem well spread on glass surface and in all cases, they clearly show a branched nature, this means that even in this case the process has been successful, even though a deeper morphological analysis should be performed, but this would be possible only with a TEM (Transmission Electron Microscope) microscope, but this was not available for this work. More information about particle dimensions and surface coverage have been retrieved thanks to ImageJ software and they are listed in table.

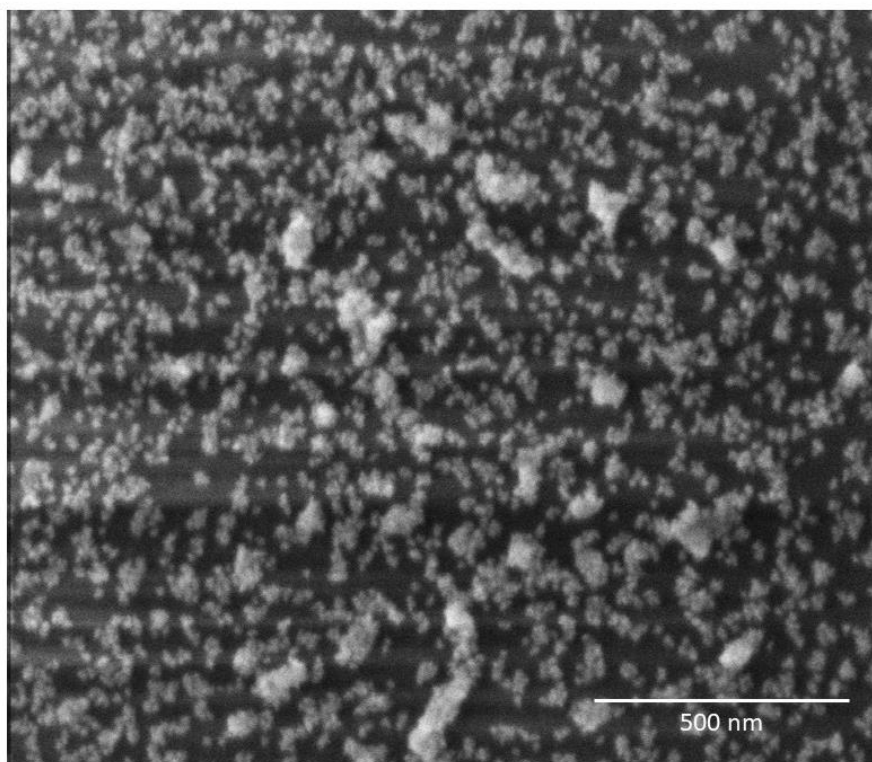


Figure 20, SEM image of 10 min Gold nanostars sample

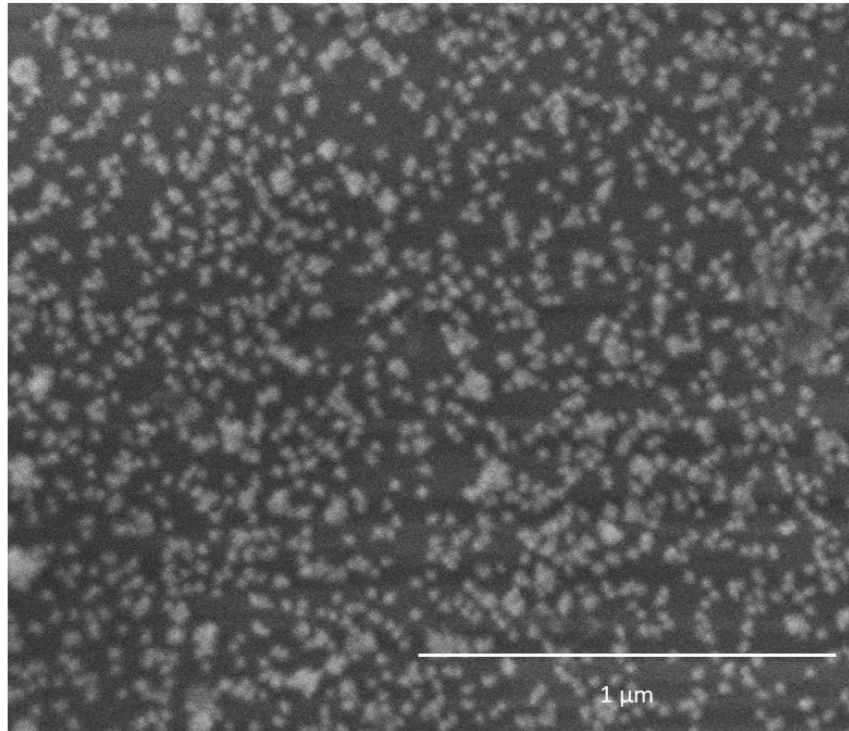


Figure 21, SEM image of 15 min Gold nanostars sample

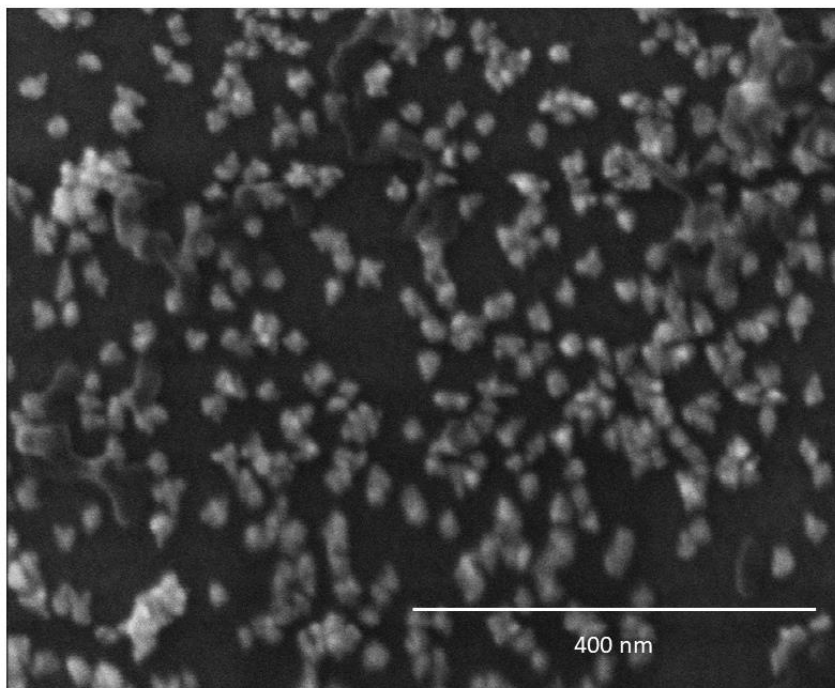


Figure 22, SEM image of 20 min Gold nanostars sample

Table 5, Average dimensions and degree of coverage of Gold nanostars

Growth time	Average dimension	Degree of coverage
10.00 min	21 nm	32 %
15.00 min	35 nm	27 %
20.00 min	37 nm	41 %

The last SEM images that are shown are those of Gold Nanoforest (fig. 23-25), in sequence there are one for each time of growth. From them it is possible to see first of all that an incredible aspect ratio have been achieved, the diameter is of some nanometers while along vertical direction they have grown for tens of nanometers, it has not been possible to measure them exactly with the means at our laboratory. Then it is possible to notice the effect of time, as it passes, the forest is always denser. As expected on top of these wires there are seeds that have undergone a certain growth, they are the white spots that could be seen in all pictures. Unfortunately, due to resolution limits and charging effect it has not been possible to achieve a better resolution as in the previous case. From the last image, the 10 min case, it is possible to see that almost all surface has been covered and top of wires is merging to start forming a uniform film. Thanks to ImageJ software it has been possible to have a measure of diameters of these wires and a rough estimate of their length and they are listed below.

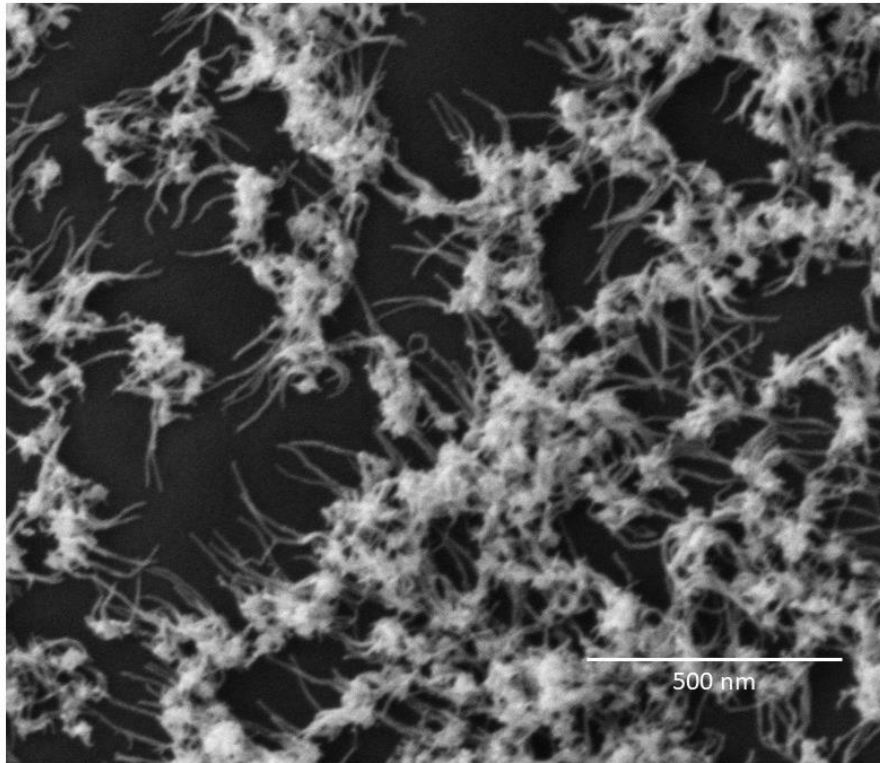


Figure 23, SEM image of 5 min Gold nanoforest sample

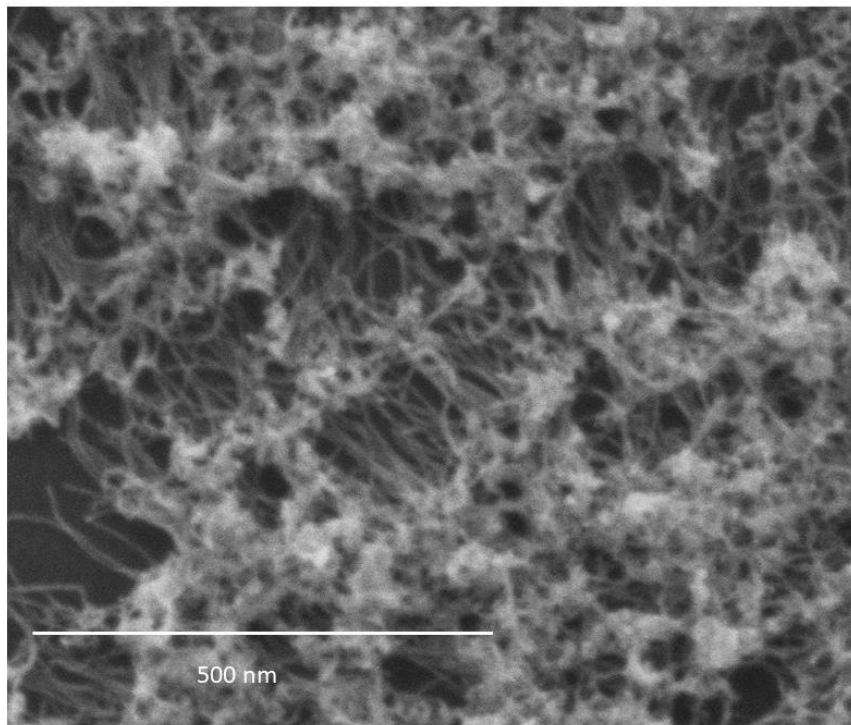


Figure 24, SEM image of 7.5 min Gold nanoforest sample

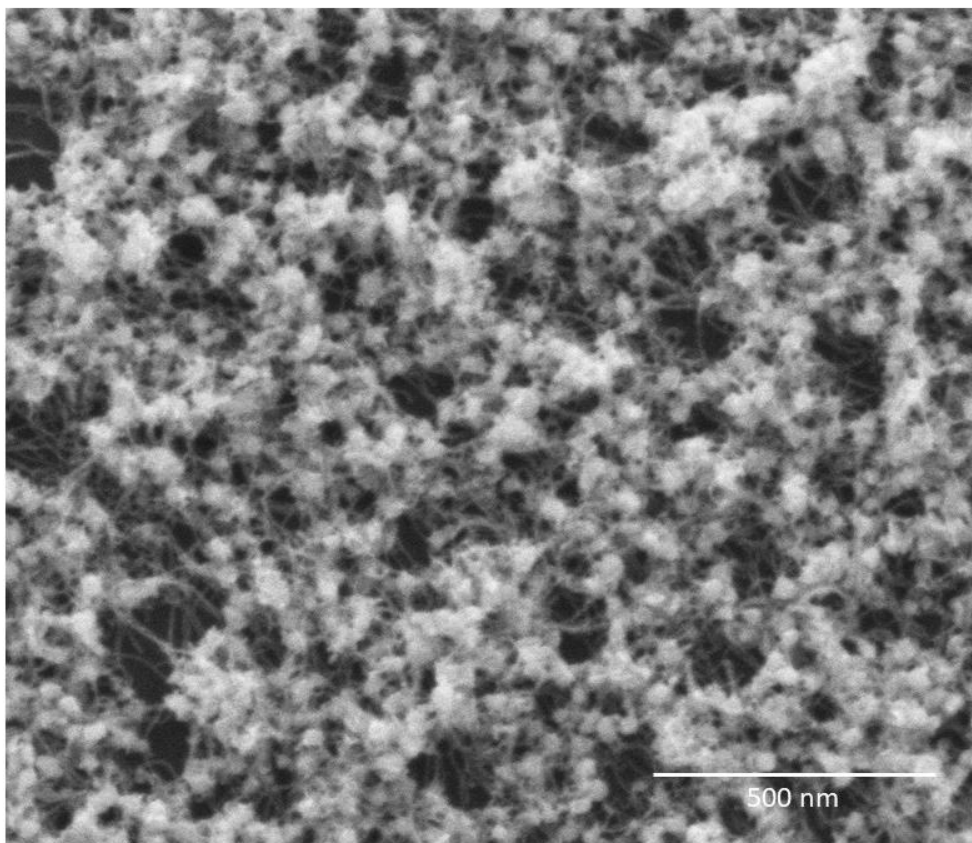


Figure 25, SEM image of 10 min Gold nanoforest sample

Table 6, Average diameter and Estimate of length for Gold Nanoforest

Growth time	Average diameter	Estimate of length
5 min	11 nm	170 nm
7.5 min	11 nm	/
10 min	13 nm	/

Finally, for what concerns gold nanoforest, due to morphology, it has not possible to determine a measure of wires. According to what expected, diameter does not grow with time because it depends on the ratio between gold and MBA. It is of 11 nm and it grows up to 13 nm in the last case; as expected, a diameter has undergone a slight growth with respect to vertical direction, taking into account that original diameter of gold seed was of 10 nm, there has been an overall growth in a range from 1 nm to 3 nm.

2.2.2 UV-visible spectroscopy

Another type of characterization that has been performed is UV-Visible spectroscopy. This technique is usually employed for characterization of gold nanoparticles because it is able to evaluate their optical properties that will depend upon their shape, dimension, surface properties, so, according to position and shape of resulting curve it is possible to have a rough estimate of shape and dimensions of nanoparticles [62-63]. For example, isotropic particles such as gold nanospheres of 10-15 nm show a peak around 535 nm, and it shifts toward higher wavelengths as their dimension increases; if they are characterized by branches, such as the nanostars, it is possible to see an important shift toward infrared wavelengths, and this behaviour is respected also in the sample that have been produced in this work.

In this case the interaction between light and nanoparticles is analysed. The technique studies the electronic transitions from ground states to excited states when matter is hit by photons. The analyser is composed by a light source and a monochromator that select the wavelength; the light beam will cross sample and light is collected by an analyser, it will measure transmitted light, and absorbance is:

$$A = \text{Log}_{10} \left(\frac{100}{T_{\%}} \right)$$

Where $T_{\%}$ is transmittance expressed as percentage of light.

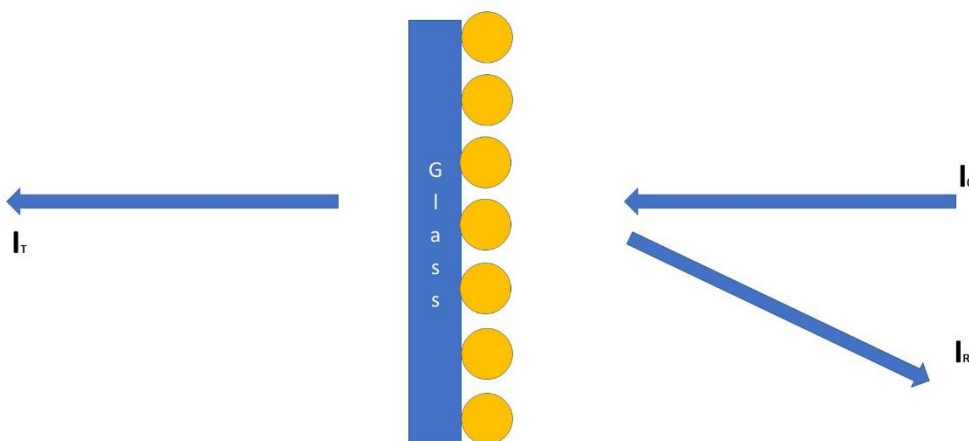


Figure 26, Light injected is partially reflected, partially transmitted and partially absorbed

With this technique it is possible to see at which wavelength Surface Plasmon Resonance happens, it is expressed as a peak in absorbance spectrum. The amplitude and position of main peak is also an indicator for particle aggregation.

UV-Visible measures have been performed at Politecnico di Torino with a Shimadzu 2600 UV-Visible spectrometer (fig. 27). The range has been set from 400 nm to 900 nm with 1 nm resolution. The system is set for analysis of liquid solutions in cuvette, so it has been necessary to modify the system in such a way it has been possible to analyse a flat solid sample. The samples have been fixed on sample holder, along light path (fig. 28).



Figure 27, UV-Visible spectrometer, Shimadzu 2600

Now results will be presented, firstly, a graph for each type of sample is shown and then a comparison between different samples, the one that show best properties for each set of samples.

All graphs have been plotted with Matlab. First measures have been imported and saved on an Excel file, then they have been processed with this software.



Figure 28, Experimental set up for UV-Visible analysis

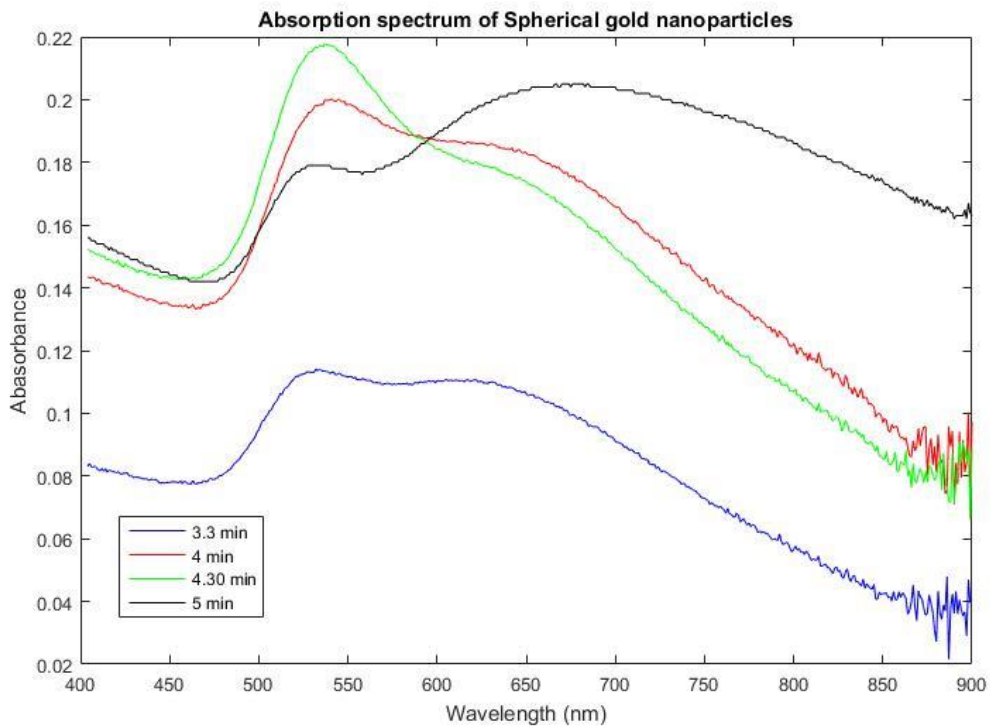


Figure 29, Absorption spectrum of gold nanospheres

From the graph (fig. 29) some consideration could be done. First of all, as expected, absorbance grows in magnitude as time passes because particles are growing, this is not true in the last case, but this will be analysed better later on. On the other side, as expected, the main peak around

535 nm, is shifted toward higher wavelengths as particles grows in dimension, this one is characteristic of spherical gold nanoparticles. Another feature that could be enlightened is the presence of another peak around 620 nm, this is not characteristic for nanospheres, but to prolonged particles. Their presence could be hardly avoided because the fabrication process is based on Brownian motion, so it is possible that a few particles undergo a different growth process, it strongly depends on seeds original shape. The fact that particles are characterized by a certain window of dimensions could be seen from how wide the main peak is. The 5 min case seems to follow a different behaviour, as it could be seen from SEM image, after 4.30 minutes, particles start merging with each other, hence there are no more only spherical nanoparticles, but the main peak is a sign that longer and oval structures are forming.

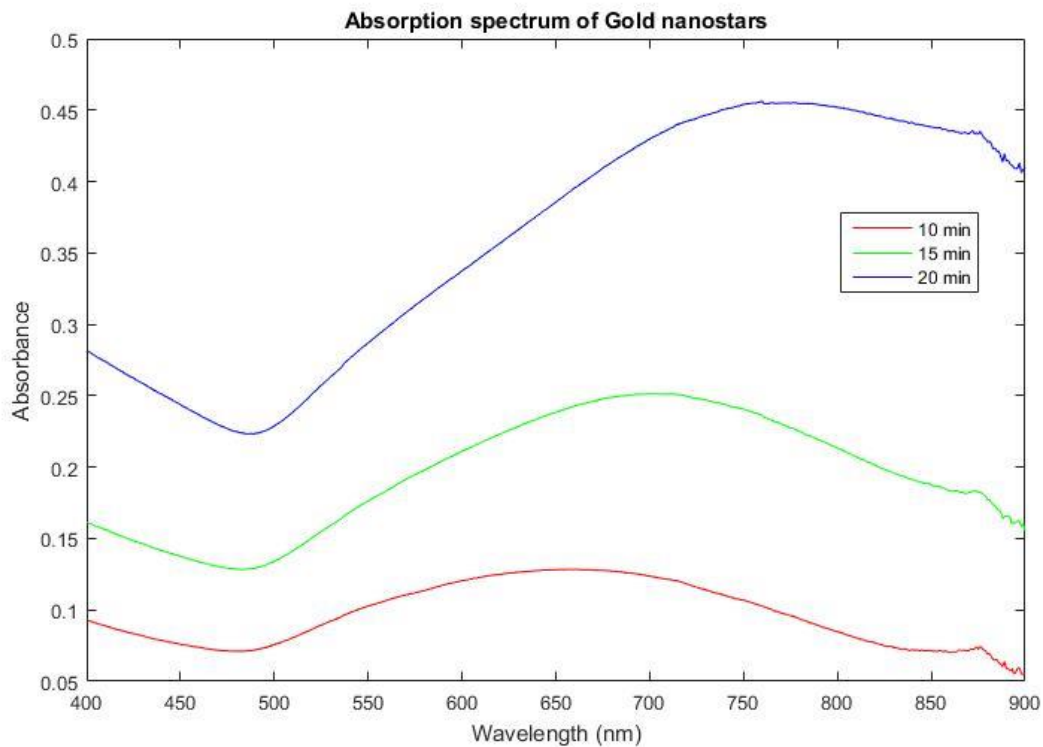


Figure 30, Absorption spectrum of Gold Nanostars

From the absorption spectrum of Gold Nanostars (fig. 30), that has been achieved with the same conditions of the previous one, it is possible to see that absorption grows as time passes as expected, because particles are bigger, moreover the main peak shifts toward infrared region. This behaviour agrees the absorption spectrum of branched nanoparticles that could be found in literature [64]. As in the previous case, due to non-uniformity of particles there is not a clear and sharp peak, but it is well spread.

For the spectrum of Gold Nanoforest (fig. 31), the same considerations for other cases are true about absorption magnitude. But some more comment is necessary; differently from the

previous samples, the absorption keep growing in the infrared region, from literature [57] in a similar case another peak is present around 1500 and 2000 nm, but it has not been possible to go so far due to instrument limitations. Moreover, a peak around 535 nm is present, as in the case of gold nanospheres, this could be addressed to gold seeds that have been lifted by the process.

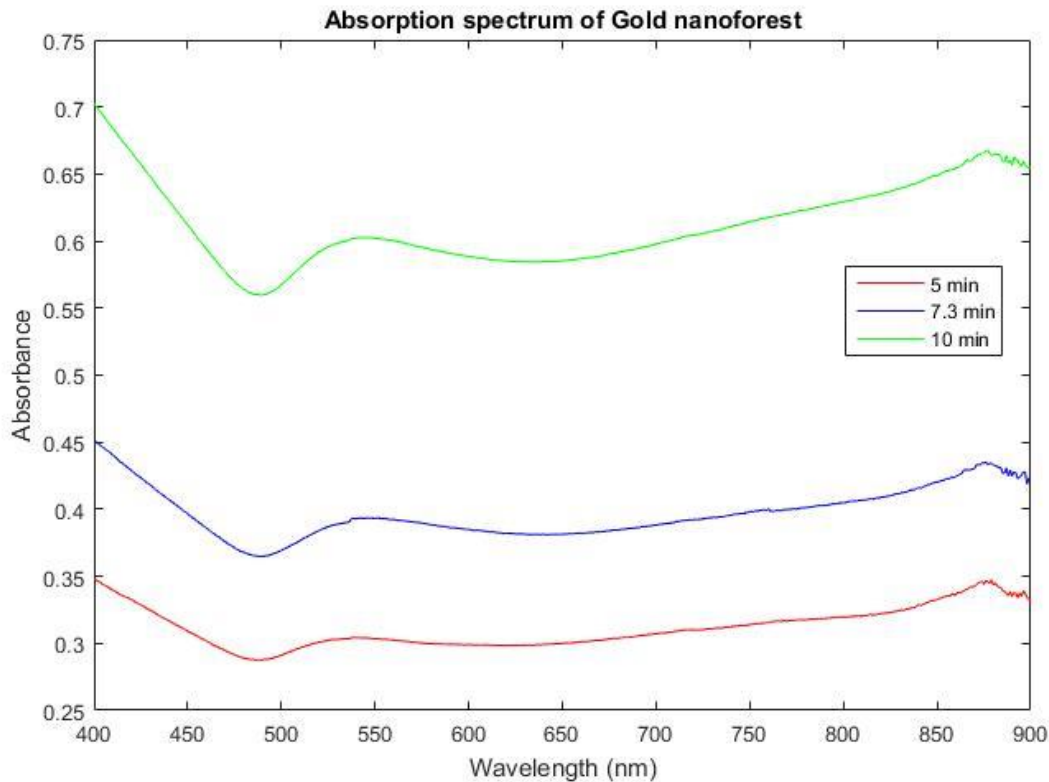


Figure 31, Absorption spectrum of Gold Nanoforest

In figure 32 a comparison between the best samples for each set is presented, so the 4.30 min for Gold Nanospheres, the 10 min sample for Gold Nanostars and the 10 min sample for Nanoforest.

The first thing is that due to different particles shape, their spectra are quite different. From a comparison between the NF and NSp spectra, in the first region there is the same peak corresponding to spherical nanoparticles; in the NF case this is due to the spherical seeds that are on top of wires, then they have completely different behaviour as stated before. Another feature is the difference in magnitude of absorption, the NSp case show the lowest one while nanoforest the higher, this could be seen also from sample with necked eye, the NF samples are of a deep grey because coverage is higher, as the NS case.

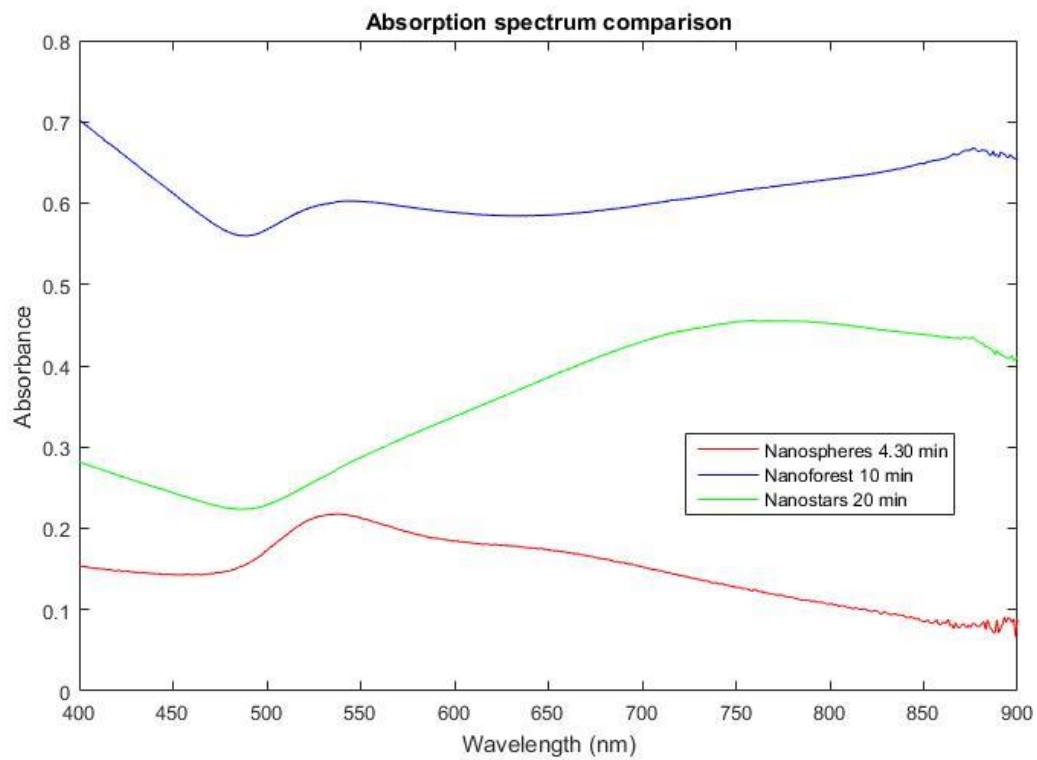


Figure 32, Comparison between absorption spectrum of Gold nanospheres, Gold nanostars and Gold nanoforest

Chapter 3, Analysis with Raman spectroscopy

3.1 Raman spectroscopy

3.1.1 Experimental conditions

The Raman measures have been carried on in a clean room at Micronova, a nanofabrication facility of Aalto University. An Alpha 300 RA spectrometer from WiTec [22] (fig. 33) has been used with 633 nm and 550 nm laser. In order to find the best measuring conditions, two different objectives have been tried, 20x and 100x. The power has been set to 1 mW. To have an average measure, 25 different measures have been registered for each sample in 25 different points and then the average has been done automatically. All samples have been previously cleaned for 5 min with a Uv-Ozone plasma cleaner at 50 W.



Figure 33, Raman spectrometer, WiTec Alpha 300 RA

Due to logistic and time issues it has been possible to test only the nanospheres samples with Thiram and Sudan III because Carbaryl was not available in Helsinki and the other substrates were not ready. In any case, following the work of Kaplas and Matikanen [23], a set of tests involving Sudan III measures have been carried on with substrates that have been patterned with a layer of Graphene. According to their studies, this layer has a significant role in enhancing Raman signal thanks to charge transfer between graphene layer and the analyte, but also, it promotes adhesion of molecules on metal substrate.

3.2 Contaminants

3.2.1 Thiram

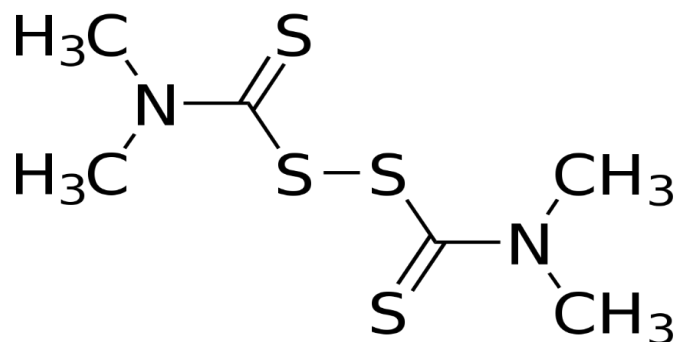


Figure 34, Thiram, PubChem

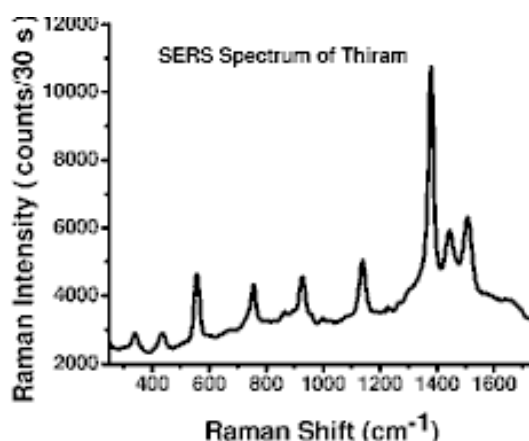


Figure 35, Thiram Raman spectrum

Thiram [13] or tetramethylthiuram disulfide is a commonly used fungicide for crop protection, but it is also used to protect harvested crops from deterioration during transport or storage. It is also found as seed protectant, but it is also an animal repellent. It is commonly used in apple and wine farming. It is characterized by a moderate toxicity if ingested while it is highly toxic if inhaled, while a repeated exposure may lead to serious problems to liver and thyroid, moreover it shows mutagenic activity that leads to chromosomic aberrations. A huge exposure leads to headaches, nausea and in general to gastrointestinal complaints. In addition to peak exposures, chronic exposure may lead to weakness, incoordinataion, slurred speech. Of major

concern is its digestion by-product, ethylene-thiourea that causes damage to the nervous system, it is considered a carcinogenic compound for humans. This is produced when Thiram is brought to high temperatures, so for example when food is cooked.

On a chemical point of view, Thiram is stable in the environment, because it has a poor solubility in water, a greater attention is necessary for ETU. It degrades faster in acidic media. In water it is degraded by hydrolysis and photocatalysis, especially under acidic conditions.

From the Raman spectrum (fig. 35) it is possible to see that there are several peaks, but the main one is around 1400 cm^{-1} .

3.2.2 Sudan III

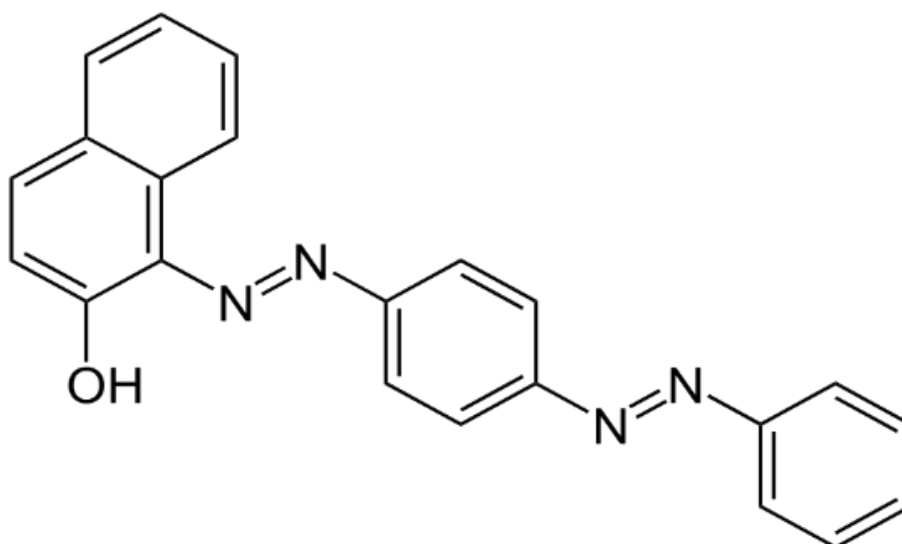


Figure 36, Sudan III

Sudan III or 1-(4-(Phenyldiazenyl)phenyl)azobenzene-2-ol [14] is one of the compounds from the family of Sudan dyes, they are used as dyes for non-polar substances such as oils, fats, as well as fuels. They cannot be used anymore as food dyes because their degradation products are known to be harmful for human health; they are proven to be genotoxic and carcinogenic. It has been banned as a dye, but it is still used illegally from some food industries; moreover, it is used also in textile industries, and as a consequence, waste water is a potential contaminant of water. One of the main causes of risk is the carcinogenic amines produced when Sudan enters the human body. It shows several Raman peaks in the range of interest (fig. 37); the main ones are at 1137 cm^{-1} and 1158 cm^{-1} .

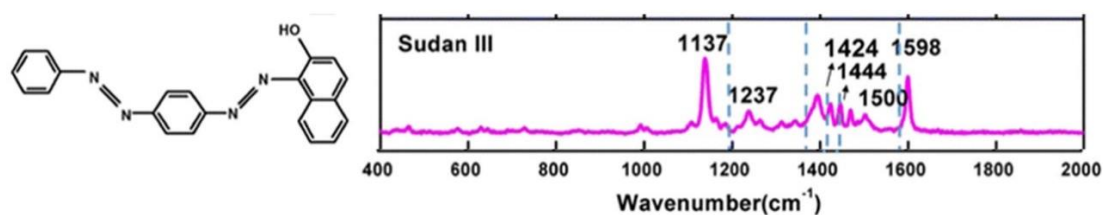


Figure 37, Raman spectrum of Sudan III

3.2.3 Carbaryl

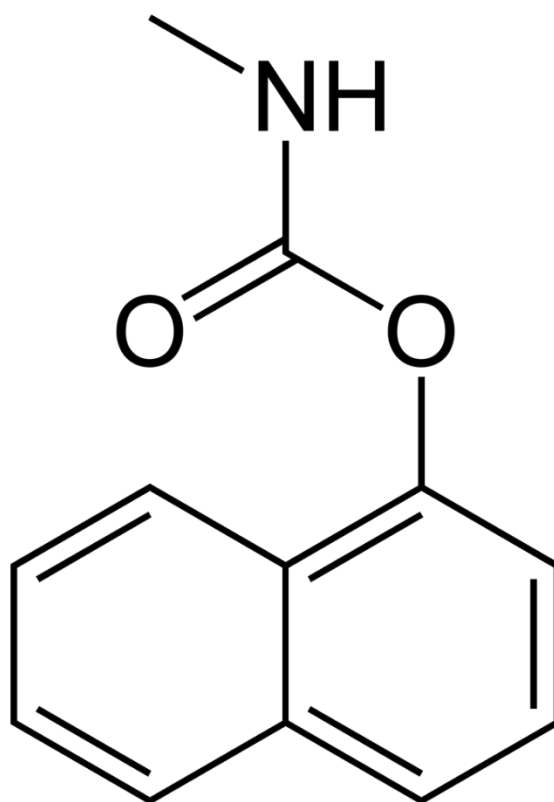


Figure 38, Carbaryl

Carbaryl or 1-naphthyl methylcarbamate [15] is an insecticide extremely common, it is used on corn, cotton, fruit as well as home yards. It could be found in low levels in surface waters and food. It could be harmful to human health after prolonged exposure, it may cause problems to nervous system, while a direct contact with skin can lead to significant irritation. Up to now it

is not considered as a potential carcinogen agent because there are no studies that prove a direct correspondence between prolonged exposure and cancer. On a physical point of view, it appears as a white and odourless crystalline solid insoluble in water. Despite it is quite safe for humans, and dangerous effects could be reversed by interrupting exposure, it is forbidden in several UE countries because it kills a great variety of insects, both dangerous and good ones.

From the Raman spectrum of Carbaryl is it possible to see several peaks, but the main one is at 1374 cm^{-1} .

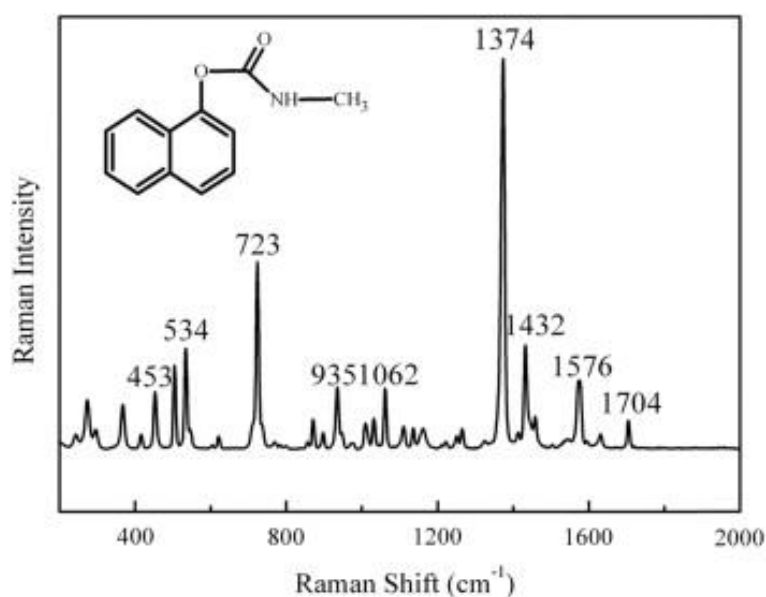


Figure 39, Raman spectrum of Carbaryl

3.3 Results

In this chapter will be shown and discussed the results achieved from Raman spectroscopy employing gold nanospheres as substrate and Thiram and Sudan III as contaminants. Firstly, the results of Thiram are described and then those for Sudan III; in this last case, it is provided also a comparison between the results achieved with simple substrate and a substrate where a layer of graphene has been deposited, so the coupled effect of SERS and GERS have been studied. As preliminary results, also Raman spectra of bare glass and the one of functionalized substrates is shown.

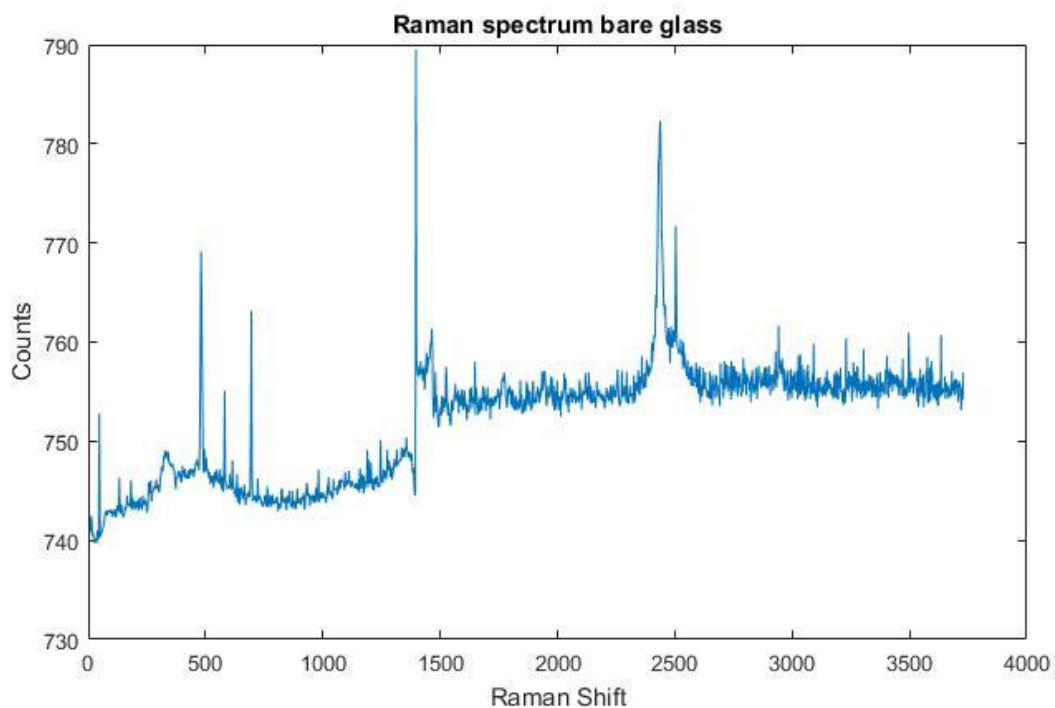


Figure 40, Raman spectrum of bare glass

Figure 40 shows the Raman spectrum of bare glass after a rapid Ozone cleaning have been performed. A characteristic peak is placed at 2500 cm^{-1} .

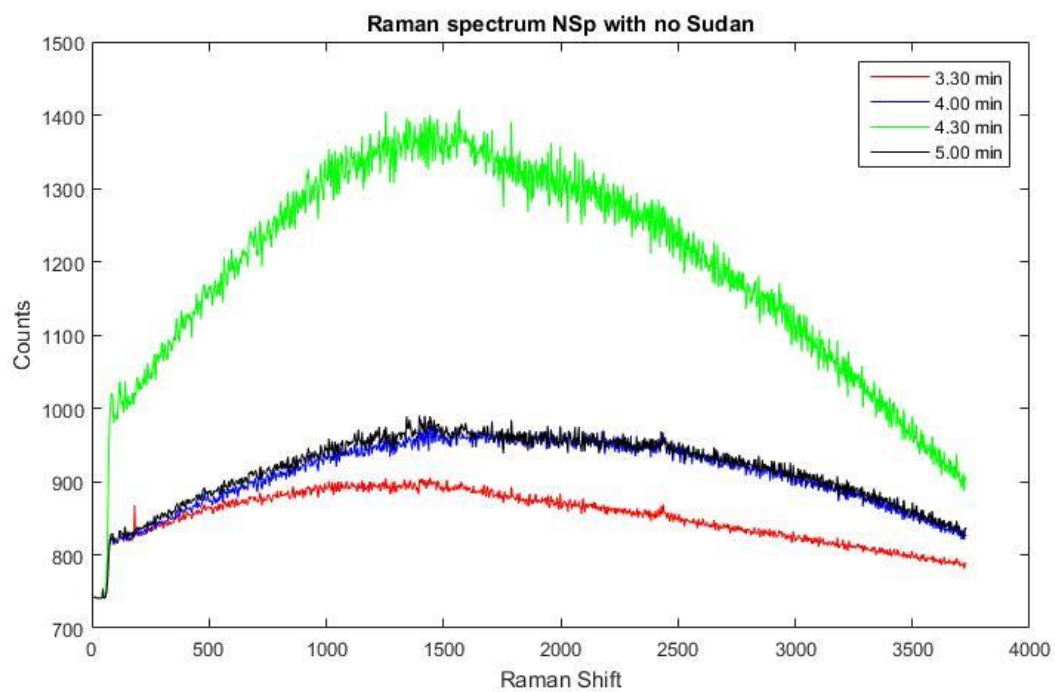


Figure 41, Raman spectra of functionalized substrates

From the picture 41, it is possible to see the Raman answer of functionalized substrates after they have been cleaned. This has been taken with a 532 nm red laser and 20x objective. The 4.30 min sample seems to have the highest response, even if a greater white noise is present. In the other cases the characteristic peak of glass is present at 2500 cm^{-1} , even if it is not really marked.

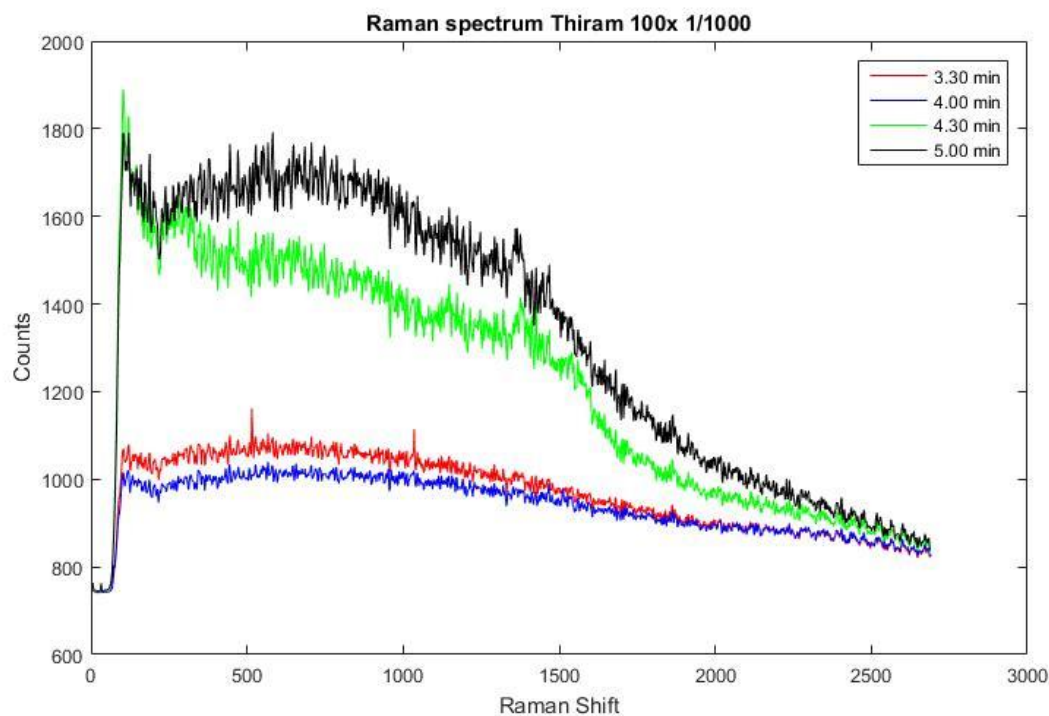


Figure 42, Raman spectrum of Thiram on several substrates at 100X, 633 nm laser

The graph 42 shows the Raman spectrum of Thiram on 4 different substrates functionalized with gold nanospheres. The data have been acquired with a 633 nm laser and objective of 100x. A solution of $20\text{ }\mu\text{M}$ of Thiram and Acetone have been tested. The solution has been poured on the samples and then Acetone have evaporated, so it has been possible to measure concentrations. In this case Thiram has been detected from 4.30 min and 5.00 min samples and this could be seen from the characteristic peak at 1380 cm^{-1} . In these cases, a huge noise is also present, this could be led to a not perfect cleaning of substrates.

The analysis has been performed also at higher concentrations, at $200\text{ }\mu\text{M}$ and 2 mM to demonstrate that signal increases as the concentration of the analyte increases. The 5 min sample has been chosen because it is the one that best performed at the lowest concentration.

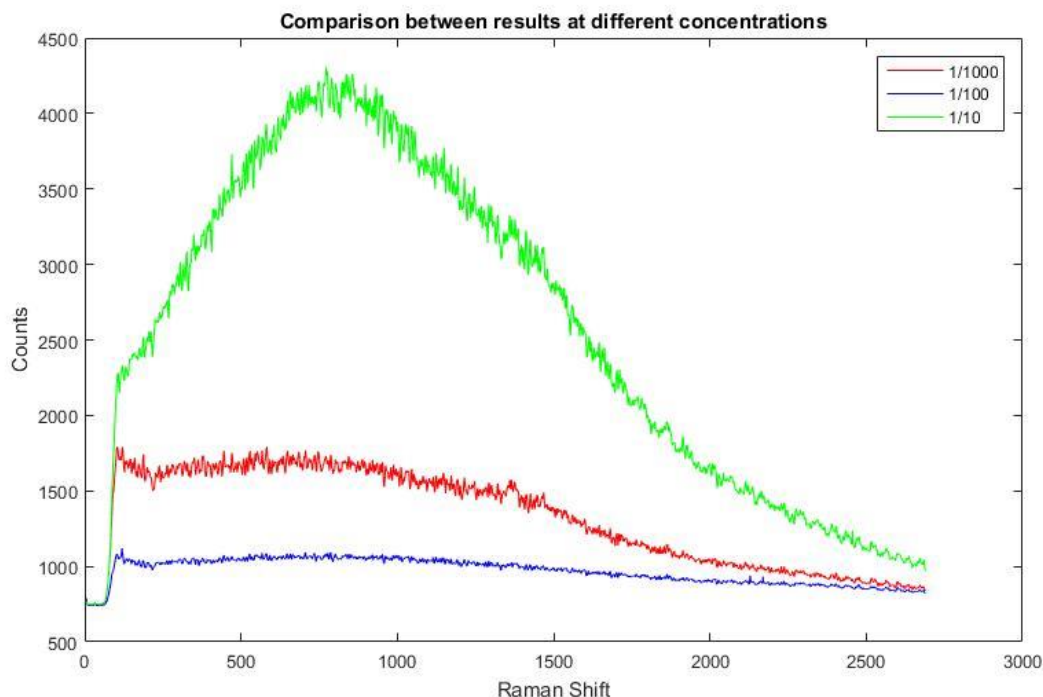


Figure 43, Raman spectrum of Thiram with different concentrations

Despite higher noise, the signal is higher when concentration is increased, and peak is well reproduced in 1/1000 and 1/10 cases. There has been a problem with 1/100 measure, the signal is flat compared to other 2 cases; this could be due to the fact that the measure has been taken on a scratch on glass, so SERS could not take place. Unfortunately, it has been possible to be aware of this only in a second moment, when measures could not be repeated anymore.

Apart from this problem, a concentration of 20 μM has been detected, that corresponds to 4.9 mg/L, which is still far from the one allowed by law, that is 0.5 $\mu\text{g/L}$, but it is a good result for a system that should perform rapid analysis so this substrate could be employed for rapid detection of Thiram in water, even if further analyses are required to understand which are the limits of detection.

Now results concerning Sudan III are presented. First those taken from substrates without any functionalization, then those with nanoparticles and finally, the results achieved employing also graphene.

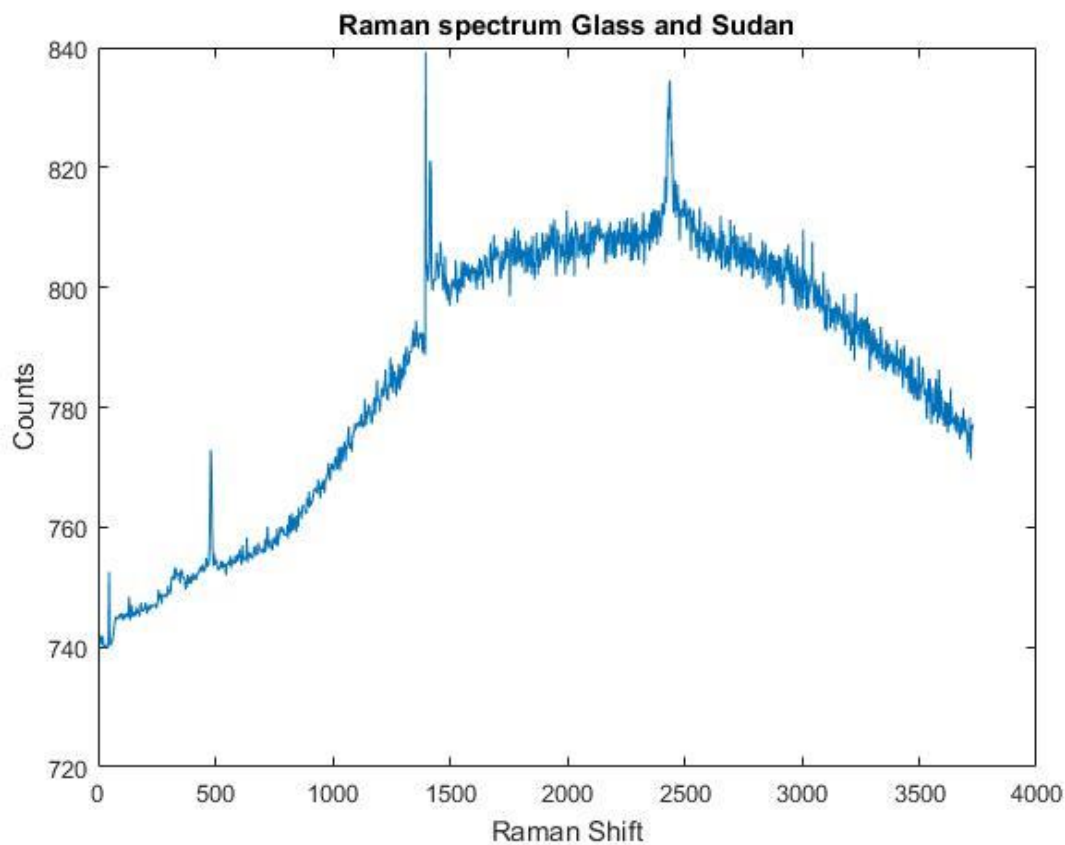


Figure 44, Raman spectrum of Sudan on bare glass

These experiments have been carried on with a solution of Sudan III 4 μM that has been prepared with Acetone. In this first case, solution has been poured on bare glass and signal has been collected with 20x objective, with 532 nm laser. There is no significant signal corresponding to Sudan III, but the one corresponding to glass is present (fig. 44).

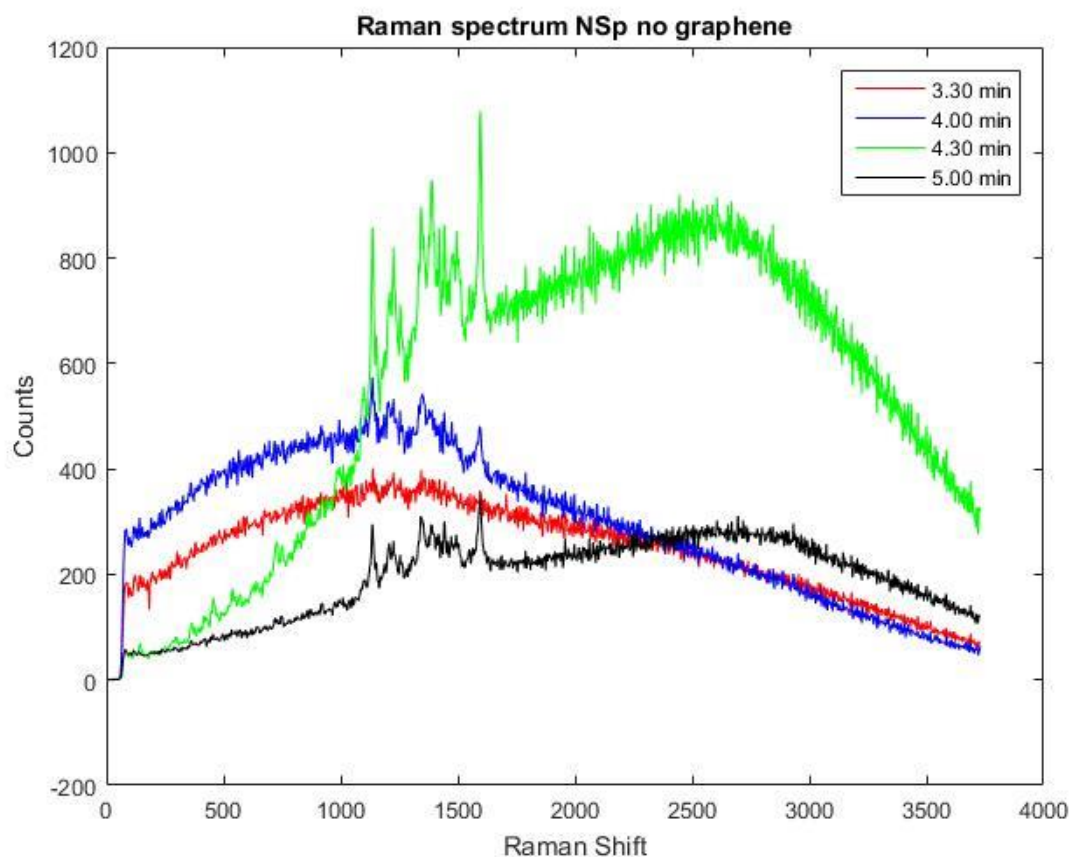


Figure 45, Raman spectrum of Sudan on gold nanosphere substrates

The picture (fig. 45) shows the answer of SERS substrates grows at different times. The characteristic Raman spectrum arises from 4.00 min sample and it is quite well remarked, especially in 4.30 min. For 5 min sample, despite low signal, the spectrum is well defined; maybe measure has been taken in a zone where there was a poor density of nanoparticles.

Now results achieved when employing also graphene are shown. Before, there is also the spectrum of Graphene achieved with it on bare glass and with Sudan on graphene, without nanoparticles.

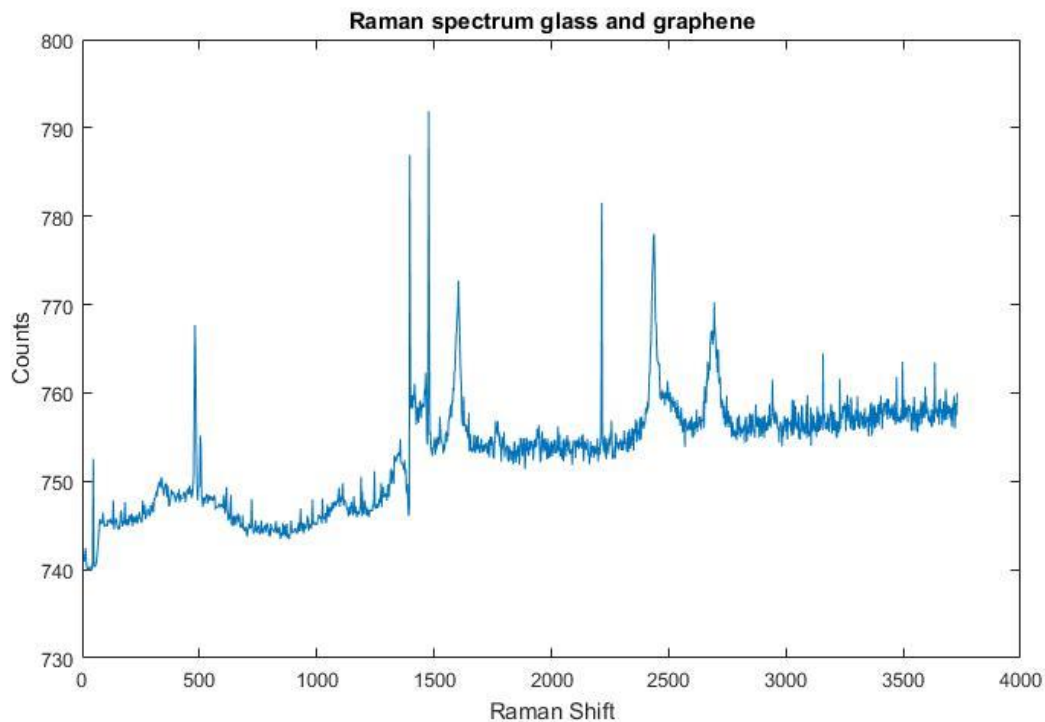


Figure 46, Raman spectrum of Graphene on glass

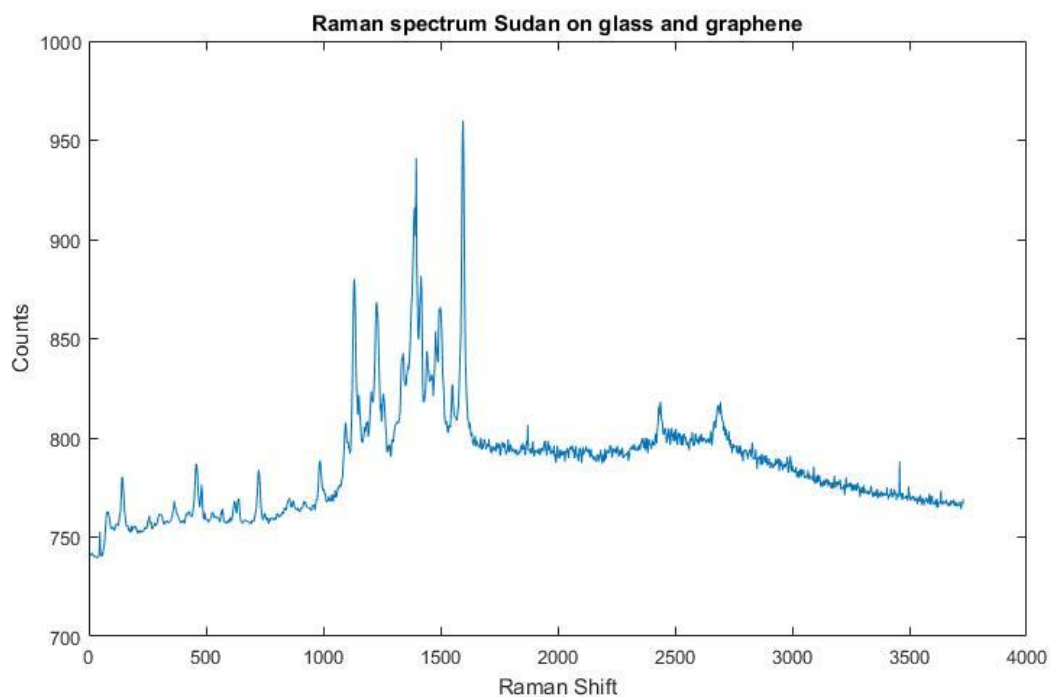


Figure 47, Raman spectrum of Sudan on graphene and bare glass

From the first picture (fig. 46), Raman spectrum of Graphene could be seen and its characteristic peaks at 2400 cm^{-1} and 2600 cm^{-1} . In the second one (fig. 47), Sudan has been analysed and its spectrum arises, this means that GERS is a worth technique for analysing this contaminant,

even if signal is not very high. On this spectrum also, graphene peaks could be noticed around 2500 cm^{-1} .

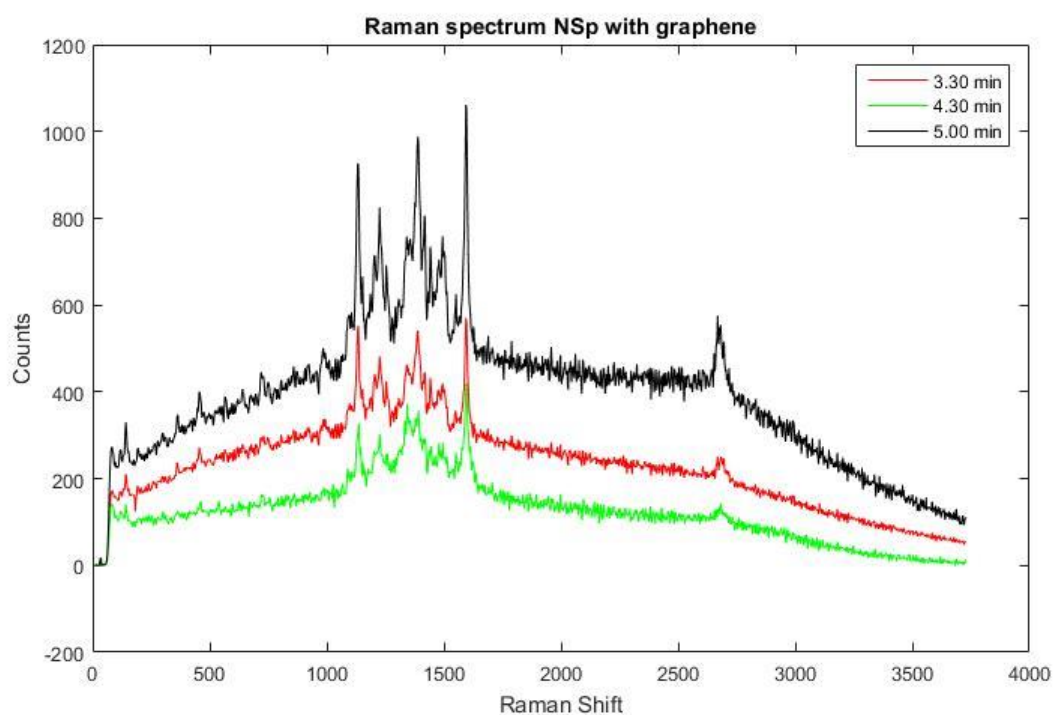


Figure 48, Raman spectrum of Sudan III on substrates functionalized with Graphene

The graph 48 depicts the Raman measurements of Sudan III on three different substrates functionalized with gold nanospheres where a layer of graphene has been deposited. 4.00 min case measure is missed. The advantage of graphene is clear, the signal could be seen also with 3.00 min case and Sudan spectrum is always well defined. In this case, 5.00 min case is the one that best performed. The presence of graphene is confirmed by the presence of a characteristic peak at 2600 cm^{-1} .

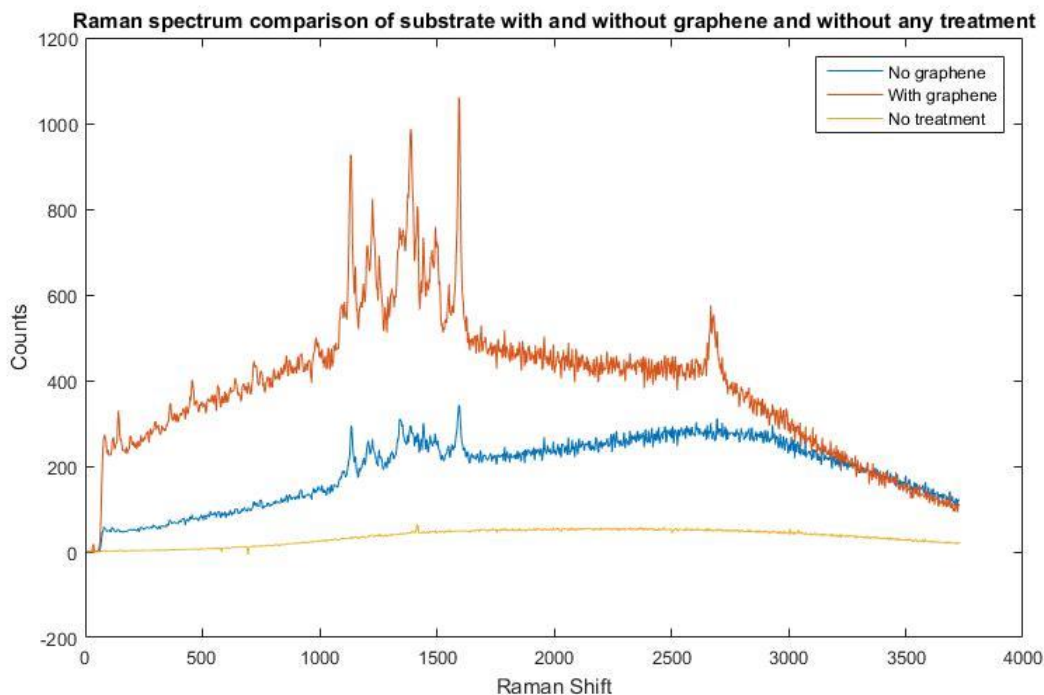


Figure 49, Comparison between Raman spectrum of Sudan III on bare glass, 5.00 min SERS substrate and functionalized graphene substrate

The last graph (fig. 49) shows a comparison between the results achieved with Sudan III on bare glass, on 5.00 min substrate and on the same substrate functionalized with a layer of graphene. Results are clear, a SERS substrate make it possible to measure a concentration of 1.4 mg/L, but signal is also improved if a layer of graphene is employed, this means that even lower concentrations could be detected, so further analysis are required to understand the Limit of Detection.

Chapter 4, Conclusions

During this work, in the framework of RaPID project, several active substrates for an optical sensor has been successfully developed. The purpose of the project is to have a fast, easy to produce and cost-effective optical sensor for monitoring water quality. Raman spectroscopy has been selected as spectroscopic technique enhanced by SERS. For this reason, 3 different types of substrates for SERS have been developed and characterized. The proposed substrates are based on gold nanospheres, gold nanostars and gold nanoforest. A first set of tests with a Raman spectrometer have been also carried on gold nanospheres.

For what concerns production process, all of them are based on wet chemistry, for this reason all are easily scalable. From cleaned bare glass, after silanization, spherical gold seeds of 10 nm are deposited and then growth process takes place; all passages could be done in just 2 days.

The growth has been tested at different times to understand which one produces the best substrate. All of them have been characterized with SEM microscopy and UV-Visible spectroscopy. They have revealed that all processes had success, and the most promising one is the nanoforest because it has produced a forest of gold nanowires that are really close, an ideal situation for SERS because there should be a high density of hotspots.

In Micronova, at Aalto University, Raman tests have started with gold nanospheres and they are promising. These substrates have been tested with Thiram and Sudan III contaminants and in both cases a concentration of around 5 mg/L has been detected, this is still high with respect to the one allowed by law that is around 0.5 $\mu\text{g/L}$. With Sudan III a further possible enhancement has been tried based on GERS, it is based on a layer of graphene on gold nanoparticles that is capable of attract more molecules, hence a better signal could be achieved, moreover it enhances Raman signal thanks to charge transfer effect.

4.1 Future work

The following step will be to validate with the proposed contaminants also the Nanostar and Nanoforest substrates. Validation should be performed by means of Raman spectroscopy with a laser at 735 nm. Nanospheres should be also tested with the same wavelength because it was not available in Helsinki; tests should be performed also with Carbaryl. A further improvement could be whether a surface treatment of gold functionalized glass may improve quality of measure. This seem promising as in the case of graphene coated spherical nanoparticles. In this case, with Sudan III, results are quite astonishing, so a set of measures also with other samples and other contaminants should be performed.

Once the best substrate will have been chosen and validated, it will be necessary to create a real working sensor, so the active substrate should be inserted in a microfluidic circuit, in such a way an operator can easily collect water and then put it the circuit, so that the analysis could be performed.

Appendix

List of chemicals and limits for EU

Table 7, List of allowed concentrations for contaminants in EU

Parameter	Parametric value	Unit
Acrylamide	0,10	µg/l
Antimony	5.0	µg/l
Arsenic	10	µg/l
Benzene	1.0	µg/l
Benzo(a)pyrene	0.010	µg/l
Boron	1.0	mg/l
Bromate	10	µg/l
Cadmium	5.0	µg/l
Chromium	50	µg/l
Copper	2.0	mg/l
Cyanide	50	µg/l
1,2-dichloroethane	3.0	µg/l
Epichlorohydrin	0.10	µg/l
Fluoride	1.5	mg/l
Lead	10	µg/l
Mercury	1.0	µg/l
Nickel	20	µg/l
Nitrate	50	mg/l
Nitrite	0.50	mg/l
Pesticides	0.10	µg/l
Pesticides-Total	0.50	µg/l
Polycyclic Aromatic hydrocarbons	0.10	µg/l
Selenium	10	µg/l
Tetrachloroethene and Trichloroethene	10	µg/l
Trihalomethanes — Total	100	µg/l
Vinyl chloride	0.50	µg/l

Preparation of Growth solutions

Gold nanospheres

The growth solution is a solution of MilliQ water and Tetrachloroauric acid at 0.28 mM with 1.75% in volume of Oxygenated water. To have 5 mL of solution it is necessary to add at the end 0.0875 μL of H_2O_2 . For gold solution, the starting one is a solution 5g/L and the final one should be 0.055 g/L. In order to obtain that, we should find the amount of mother solution to dissolve in 5 mL of MilliQ water to obtain a solution 0.28 mM.

$$m_{Au} = M * V_{fin} * MW = 0.28 \text{ mM} * 5\text{mL} * 250.96 \text{ u} = 351 \mu\text{g}$$

$$V_{Au} = m_{Au} * \frac{V_{Au \text{ mother}}}{m_{Au \text{ mother}}} = 70 \mu\text{L}$$

Firstly, the solution with water and gold should be prepared, then the glass sample has to be inserted, then it is necessary to start stirring the solution, finally, oxygenated water needs to be added so that reactions could start, time should start now; stirring should be kept during all reaction time.

Gold Nanostars

Now it will be described the procedure to obtain the growth solution for Gold nanostars. It is based on a solution of PVP in DMF 10 mM and HAuCl_4 at 50 mM.

PVP is sold in powder, so it is necessary to compute the mass of PVP that is necessary to obtain the solution.

$$m_{PVP} = M * V_{fin} * MW = 10 \text{ mM} * 5\text{mL} * 10000 \text{ u} = 0.5 \text{ g}$$

Then the solution is formed, and it is necessary to stir it for some minute to have a uniform one. After that the gold solution should be prepared. The starting one is Tetrachloroauric acid at

3.9g/mL and we want 5 mL of solution in MilliQ water at 50 mM. In this case the gold source is so dense that it is solid.

$$m_{Au} = M * V_{fin} * MW = 50 \text{ mM} * 5\text{mL} * 250.96 \text{ u} = 63 \text{ mg}$$

So, it will be necessary to weight this amount of gold, it will solve almost immediately when in water. Then 27 μ L of this solution should be added to the previous one.

After preparing the DMF and PVP solution, the sample, once cleaned, could be immersed; after this, it is necessary to start stirring the solution, then gold solution could be added, reaction time should be start at this moment, while stirring has to be kept during all the process.

Gold Nanoforest

For what concerns the production of a gold nanoforest, the process involves several chemicals that should be prepared before. The final solution should be composed from 3:1 Ethanol and MilliQ water in volume. Then it should be 550 μ M of MBA, 1.7 mM of HAuCl₄ and finally 4.1 mM of L-AA.

Starting from the solvents, to have 4 mL of final solution, 0.3852 mL of MilliQ water and 2.960 mL of Ethanol are mixed. Then, a solution of 40mL of Ethanol and MBA is prepared; MBA is sold in powder, so it is necessary to find the mass to solve in 4 mL to obtain a solution 55 mM and then another dilution to reach 550 μ M:

$$m_{MBA} = M * V_{fin} * MW = 55 \text{ mM} * 40\text{mL} * 154.183 \text{ u} = 339 \text{ mg}$$

Then the solution has to be stirred for several minutes to have a uniform one; it is necessary to compute the amount to obtain the 550 μ M solution in 4 mL:

$$m_{MBA} = M * V_{fin} * MW = 550 \text{ } \mu\text{M} * 4\text{mL} * 154.183 \text{ u} = 339 \text{ } \mu\text{g}$$

And so:

$$V_{MBA} = m_{MBA} * \frac{V_{MBA \text{ mother}}}{m_{MBA \text{ mother}}} = 40 \text{ } \mu\text{L}$$

The same thing should be done with L-AA. It is solved before in 4 mL of MilliQ water to reach a concentration of 410 mM and then it is solved again to reach the desired concentration.

$$m_{L-AA} = M * V_{fin} * MW = 410 \text{ mM} * 4\text{mL} * 176.124 \text{ u} = 289 \text{ mg}$$

Appendix

$$m_{L-AA} = M * V_{fin} * MW = 4.1 \text{ mM} * 4\text{mL} * 176.124 \text{ u} = 2.89 \text{ mg}$$

So, it is necessary to take the following amount:

$$V_{L-AA} = m_{L-AA} * \frac{V_{L-AA}}{m_{L-AA}} = 40 \mu\text{L}$$

Finally, the gold solution should be prepared. The starting one is the same for nanostars, so 3.9 g/ml, but now a solution of 1.7 mM is required. Firstly, 39 mg of tetrachloroauric acid is diluted in 1 mL of water, then the mass of gold required is computed:

$$m_{Au} = M * V_{fin} * MW = 1.7 \text{ mM} * 4\text{mL} * 250.96 \text{ u} = 1.7 \text{ mg}$$

And finally, the amount of mother solution to reach the required concentration:

$$V_{Au} = m_{Au} * \frac{V_{Au \text{ mother}}}{m_{Au \text{ mother}}} = 578 \mu\text{L}$$

After all reagents have been prepared, gold solution could be added to Water-Ethanol solution; after that, cleaned samples could be immersed in the falcon and stirring could start, at this stage MBA and L-AA could be added, in this order and time could start running. In this case stirring is required for the first seconds, 30 s is enough.

Bibliography

- [1] NATO. (n.d.). <https://maps-polito.com/wp/rapid-project/>.
- [2] World Health Organization. (2011). Guidelines for drinking-water quality, 4. e. (n.d.).
- [3] DIRECTIVE 2000/60/EC OF THE EUROPEAN PARLIAMENT AND OF THE COUNCIL of 23 October 2000 establishing a framework for Community action in the field of water policy.
- [4] COUNCIL DIRECTIVE 98/83/EC of 3 November 1998 on the quality of water intended for human consumption
- [5] <http://www.chem.ucla.edu/~bacher/General/30BL/gc/theory.html>
- [6] Branched metal nanoparticles: a review on wet-chemical synthesis and biomedical applications, Si Yue li and Min Wang
- [7] Colleen L. Nehl, Hongwai Liao, Optical Properties of Star-Shaped Gold Nanoparticles, Nanoletters, Huston, 2006
- [8] Tapan k. Sau and Catherine J. Murphy, Room Temperature, High-Yield Synthesis of Multiple Shapes of Gold Nanoparticles in Aqueous Solution, JACS Communications, South Carolina, 2004
- [9] Piranha Solution Information & Safety: Ortiz Lab 03/04, MIT
- [10] Biswa Ranjan Panda¹ and Arun Chattopadhyay, Synthesis of Au Nanoparticles at “all” pH by H₂O₂ Reduction of H₂AuCl₄, ASP, Guwahati, 2007
- [11] Xiaokong Liu, Haolan Xu, Rapid Seeded Growth of Monodisperse, Quasi-Spherical, Citrate-Stabilized Gold Nanoparticles via H₂O₂ Reduction, Langmuir, Jinan, 2012
- [12] Nan Jiang, Tip-enhanced Raman spectroscopy: From concepts to practical applications, Elsevier, Chicago, 2016
- [13] pmep.cce.cornell.edu/profiles/extoxnet/pyrethrins-ziram/thiram-ext.html
- [14] Fonovich TM, Sudan dyes: are they dangerous for human health?, PubMed, Bueno Aires, 2013

Bibliography

- [15] <http://www.epa.gov/sites/production/files/2016-09/documents/carbaryl.pdf>
- [16] New SERS substrate fabrication by nano-assembly techniques, 2014, Karl Meissner
- [17] Xiaokong Liu, Haolan Xu, Rapid Seeded Growth of Monodisperse, Quasi-Spherical, Citrate-Stabilized Gold Nanoparticles via H₂O₂ Reduction, *Langmuir*, Jinan, 2012
- [18] <https://www.cytodiagnosics.com/store/pc/Introduction-to-Gold-Nanoparticle-Characterization-d3.htm>
- [19] Pandian Senthil Kumar, Isabel Pastoriza-Santos, High-yield synthesis and optical response of gold nanostars, IQP Publishing, Vigo, 2007
- [20] Jiating He, Yawen Wang, Forest of Gold Nanowires: A New Type of Nanocrystal Growth, ACS publications, Singapore, 2013
- [21] <https://imagej.net/Welcome>
- [22] <https://www.witec.de/products/raman-microscopes/alpha300-r-confocal-raman-imaging/>
- [23] Tommi Kaplas, Antti Matikainen, Scalable fabrication of the graphitic substrates for graphene-enhanced Raman spectroscopy, *Nature*, Joensuu, 2017
- [24] W. Kiefer, *Surface Enhanced Raman Spectroscopy*, Wiley-VCH, Weinheim, 2011.
- [25] M. Fleischmann, P. Hendra, and A. McQuillan, "Raman spectra of pyridine adsorbed at a silver electrode," *Chemical Physics Letters*, vol. 26, no. 2, pp. 163–166, 1974.
- [26] Maher R.C. (2012) SERS Hot Spots. In: Kumar C.S.S.R. (eds) *Raman Spectroscopy for Nanomaterials Characterization*. Springer, Berlin, Heidelberg
- [27] D. L. Jeanmaire and R. P. V. Duyne, "Surface Raman spectroelectrochemistry: Part i. heterocyclic, aromatic, and aliphatic amines adsorbed on the anodized silver electrode," *Journal of Electroanalytical Chemistry and Interfacial Electrochemistry*, vol. 84, no. 1, pp. 1–20, 1977.
- [28] S. Nie and S. R. Emory, "Probing single molecules and single nanoparticles by surface-enhanced raman scattering," *Science*, vol. 275, no. 5303, pp. 1102–1106, 1997.
- [29] S. Schlucker, "Surface-enhanced Raman spectroscopy: Concepts and chemical applications," *Angewandte Chemie International Edition*, vol. 53, no. 19, pp. 4756–4795, 2014.
- [30] P. Larkin, *Infrared and Raman Spectroscopy; Principles and Spectral Interpretation*. Elsevier Science, 2011.

Bibliography

- [31] Javier Reguera, Judith Langer, Anisotropic metal nanoparticles for surface enhanced Raman scattering; Chemical Society Reviews, 2017
- [32] Robert Loos, Bernd Manfred Gawlik, EU-wide survey of polar organic persistent pollutants in European river waters, Elsevier, Ispra, 2008
- [33] D.J. Lapworth, N. Baran, Emerging organic contaminants in groundwater: A review of sources, fate and occurrence, Elsevier, Oxfordshire, 2012
- [34] <https://www.who.int/>
- [35] <https://www.who.int/whopes/resources/en/>
- [36] C. V. Raman, A new type of secondary emission, Nature, Calcutta, 1928
- [37] <https://www.renishaw.com/en/why-we-use-raman-spectroscopy--25803>
- [38] Michael M. Cerrabba, Robert B. Edmonds, Feasibility studies for the detection of organic surface and subsurface water contaminants by surface-enhanced Raman spectroscopy on silver electrodes, ACS publications, Massachusetts, 1987
- [39] Nannan Sun, Kaisheng Yao, Synthesis of various gold hierarchical architectures assisted by functionalized ionic liquids in aqueous solutions and their efficient SERS responses, Elsevier, Luoyang, 2018
- [40] Na Li, Pengxiang Zhao, Anisotropic Gold Nanoparticles: Synthesis, Properties, Applications, and Toxicity, Wiley-VCH, Talence Cedex, 2014
- [41] Ser-Sing Chang, Chien-Liang Lee, Gold Nanorods: Electrochemical Synthesis and Optical Properties, ACS Publications, Taiwan, 1997
- [42] Nikhil R. Jana, Catherine J. Murphy, Wet Chemical Synthesis of High Aspect Ratio Cylindrical Gold Nanorods, ACS Publications, Columbia, 2001
- [43] Y. Maeda, H. Tabata, Two-dimensional assembly of gold nanoparticles with a DNA network template, Applied Physics, Osaka, 2001
- [44] H. Wang, N.J. Halas, Mesoscopic Au "Meatball" Particles, Advanced Materials, 2008
- [45] Jianping Xie, Qingbo Zhang, The Synthesis of SERS-Active Gold Nanoflower Tags for In Vivo Applications, ACS publications, Singapore, 2008

Bibliography

- [46] Shaojun Guo, Erkang Wang, Synthesis and electrochemical applications of gold nanoparticles, Elsevier, Jilin, 2007
- [47] J.J. Crass, C.A. Rowe Taitt, Comparison of chemical cleaning methods of glass in preparation for silanization, Elsevier, Washington DC, 1999
- [48] J. C. Love, L. A. Estroff, J. K. Kriebel, R. G. Nuzzo, and G. M. Whitesides, "Self-assembled monolayers of thiolates on metals as a form of nanotechnology," *Chemical Reviews*, vol. 105, no. 4, pp. 1103–1170, 2005.
- [49] D. K. Schwartz, "Mechanisms and kinetics of self-assembled monolayer formation," *Annual Review of Physical Chemistry*, vol. 52, no. 1, pp. 107–137, 2001. PMID: 11326061.
- [50] S. Barlow and R. Raval, "Complex organic molecules at metal surfaces: bonding, organisation and chirality," *Surface Science Reports*, vol. 50, no. 6–8, pp. 201 – 341, 2003.
- [51] F. Schreiber, "Structure and growth of self-assembling monolayers," *Progress in Surface Science*, vol. 65, pp. 151–257, Nov. 2000.
- [52] J. B. Brzoska I. Ben Azouz, Silanization of Solid Substrates: A Step toward Reproducibility, Langmuir, Paris, 1994
- [53] Mojun Zhu, Maria Z. Lerum, How to Prepare Reproducible, Homogeneous, and Hydrolytically Stable Aminosilane-derived Layers on Silica, Langmuir, South Hadley, 2012
- [54] www.sigmaaldrich.com/technical-documents/articles/materials-science/nanomaterials/gold-nanoparticles.html
- [55] Biswa Ranjan Panda and Arun Chattopadhyay, Synthesis of Au Nanoparticles at "all" pH by H₂O₂ Reduction of H_{Au}Cl₄, ASP, Guwahati, 2007
- [56] Isabel Pastoriza-Santos, Luis M. Liz-Marzan Formation of PVP-Protected Metal Nanoparticles in DMF, Langmuir, Vigo, 2002
- [57] Andrea La Porta, Marek Grzelczak, Gold Nanowire Forests for SERS Detection, Wiley-VCH, Donostia-San Sebastián, 2014
- [58] Oliver C. Wells, Scanning electron microscopy, McGraw-Hill, 1974
- [59] A. Alyamani, O. M. Lemine, FE-SEM Characterization of Some Nanomaterial, IntechOpen, 2012

Bibliography

- [60] Ki Hyun Kim, Zentaro Akase, Charging Effects on SEM/SIM Contrast of Metal/Insulator System in Various Metallic Coating Conditions, Materials Transaction, Tohoku, 2010
- [61] Shimadzu UV-2600 Spectrometer Operation Guide, University of York
- [62] Sanim Rahman, Size and Concentration Analysis of Gold Nanoparticles With Ultraviolet-Visible Spectroscopy, UJMM, 2016
- [63] Wolfgang Haiss, Nguyen T. K. Thanh, Determination of Size and Concentration of Gold Nanoparticles from UV-Vis Spectra, Analytical Chemistry, Liverpool, 2007
- [64] Peter N. Njoki, I-Im S. Lim, Size Correlation of Optical and Spectroscopic Properties for Gold Nanoparticles, ACS publications, Binghamton, 2007

Acknowledgements

I would like to conclude this work by expressing the sincerest thanks to all people that believed in me and supported me during these years, without them, I would not have overcome lot of difficulties I have encountered during this path.

First of all, I want to remember prof. Davide Janner that allowed me to take part in RaPID project and I wish to thank him for his precious guide and advices that during these months have been essential for the advance of the thesis. A special thank goes to Doct. Elisa Muzi and Doct. Diego Pugliese that have supervised my work since the beginning, they have been always available and thanks to their experience I have learned how to move in a chemical laboratory and much more. I would like to remember also Doct. Antti Matikainen that helped me with measures during the period I have spent in Helsinki, at Aalto University.

Some special thanks go to my family, my mother Nunzia, my father Franco and my brother Federico, they saw me to leave several years ago and their support has never lacked. I hope this little joy will repay them a bit for all they have done for me, for all concerns and anxiety of these years. Thanks also to all my relatives that make every holiday special.

During these years I have lived at Collegio Einaudi, there, I have found another family, made of people from all over Italy and Europe, and I want to thank all of them because they make me feel at home every time I come back in Turin. It would be hard to name them all, but I am grateful especially to those that I have encountered during the first years, because they have made these years more interesting and fuller of experiences, from travels around Europe to mountains climbing, from gym to concerts. Thanks also to my mates, especially to Federico, all the days and nights spent on PCs will be unforgettable.

Thanks also to all my friends from Martina, every time I came home it seemed that we have always been together, even if we have been apart for months.

Finally, I would like to share a special thanks to Elvira, my girlfriend, she has been always at my side during these years, she always supported and encouraged me to do the best and I am extremely thankful to her for the precious help she gave me while writing this thesis.